

Mechanisms for Primordial Black Hole Production in String Theory

Ogan Özsoy[♣], Susha Parameswaran[♠], Gianmassimo Tasinato[♣], Ivonne Zavala[♣]

[♣] *College of Science, Swansea University, Swansea, SA2 8PP, UK*

[♠] *Department of Mathematical Sciences, University of Liverpool, Liverpool, L69 7ZL, UK*

Abstract

We consider mechanisms for producing a significant population of primordial black holes (PBHs) within string inspired single field models of inflation. The production of PBHs requires a large amplification in the power spectrum of curvature perturbations between scales associated with CMB and PBH formation. In principle, this can be achieved by temporarily breaking the slow-roll conditions during inflation. In this work, we identify two string setups that can realise this process. In string axion models of inflation, sub-leading non-perturbative effects can superimpose steep cliffs and gentle plateaus onto the leading axion potential. The cliffs can momentarily violate the slow-roll conditions, and the plateaus can lead to phases of ultra slow-roll inflation. We thus achieve a string motivated model which both matches the Planck observations at CMB scales and produces a population of light PBHs, which can account for an order one fraction of dark matter. In DBI models of inflation, a sharp increase in the speed of sound sourced by a steep downward step in the warp factor can drive the amplification. In this scenario, discovery of PBHs could indicate non-trivial dynamics in the bulk, such as flux-antibrane annihilation at the tip of a warped throat.

Contents

1	Introduction	2
2	Enhancing the amplitude of curvature fluctuations in single field inflation	4
3	PBHs in axion inflation with subleading non-perturbative effects	6
3.1	Bumpy inflation	7
3.2	Background evolution – slow roll, fast roll	8
3.3	Ultra slow-roll phase	10
3.4	Phenomenology at CMB scales	12
3.5	Amplification of curvature perturbations at small scales	16
3.6	PBHs from non-perturbative effects in axion inflation	17
3.6.1	Observational constraints on PBH abundance	21
3.6.2	Implications for reheating	22
4	DBI inflation with steps in the warp factor	23
4.1	Background and perturbations with non-canonical kinetic terms	24
4.2	Enhancement of curvature fluctuations in DBI inflation	25
5	Conclusions	28
	References	31

1 Introduction

In the early 1970s, Stephen Hawking proposed that overdense inhomogeneities in the very early Universe could gravitationally collapse to form Primordial Black Holes (PBHs) [1, 2]. Assuming the Planck length as the minimal possible Schwarzschild radius, gives a lower limit for black holes masses of about $10^{-5}g$. Moreover, this mechanism – in contrast to the astrophysical process from dying stars – allows for populations of black holes spanning a vast range of masses, from the Planck scale to supermassive and beyond. Constraints on PBHs abundances continue to improve, but leave viable windows, especially when astrophysical uncertainties are taken into account (see [3, 4] for recent reviews).

PBHs could provide a significant fraction – or indeed all – of the mysterious Dark Matter that dominates cosmic structures in the present day Universe. Stimulated both by the absence of signatures for well-motivated particle candidates for Dark Matter and by the first detection of gravity waves from merging black holes, this idea has recently taken new flight. The principal modern process for PBH production is the collapse of curvature perturbations generated during early Universe cosmic inflation, when the relevant scales re-enter the horizon during the radiation era [5]. However, the big challenge here is that the amplitude of these inflationary curvature perturbations at the large scales probed by the CMB has been constrained by observations to be tiny, $A_s \sim 10^{-9}$ at the pivot scale $k = 0.05 \text{ Mpc}^{-1}$. In order for inflationary perturbations to lead to a significant PBH population there must be some mechanism at work that enhances the power spectrum to around $A_s \sim 10^{-2}$ at some smaller scale. For example, a large enhancement at scales around $k \sim 10^{12} - 10^{14} \text{ Mpc}^{-1}$ would lead to PBHs masses in the window $10^{-17}M_\odot \lesssim M_{PBH} \lesssim 10^{-13}M_\odot$, which could be a dominant component of Dark Matter consistently with current observational constraints¹.

Many recent works have explored how such an enhancement could be achieved. As current CMB observations are consistent with the simplest, single field slow-roll models, much of the focus has been to explore scenarios producing PBHs in single field inflation [7–11]. A possibility is that the inflaton rolls down a slow-roll plateau, probed by the CMB observations, followed by a near-inflection point which leads to a phase of ultra slow-roll. Roughly, the extreme flattening of the inflationary potential around the inflection point leads to an enhanced amplitude of scalar perturbations. Whilst such a potential can certainly be manufactured within effective field theory, ultimately its shape – and robustness against quantum corrections – would have to be explained within a fundamental theory, like string theory. For example, an attempt towards embedding this model within string theory via fine-tuned string-loop corrections in fibre inflation has been made very recently in [12], although it has not yet proved possible to fine-tune a setup such that cosmological

¹A possible obstacle for PBH's as Dark Matter in this mass range is the constraints arise due to capture of PBH by stars during their formation which may limit the PBH abundance to no more than one percent of the Dark Matter density [6].

perturbations both match the CMB and produce significant PBH Dark Matter.

The purpose of this paper is to identify well-motivated string mechanisms that can lead to an amplification of curvature perturbations and thus significant PBH production in the early Universe. To do so, it is helpful to recall the physical conditions underlying this amplification, first discussed by Leach et al. [13, 14]². In slow-roll inflation, the equation that governs the curvature perturbation takes the form of a damped harmonic oscillator. Solutions for super-horizon modes correspond to a linear combination of a constant and a decaying mode. However, if the slow-roll conditions are broken, then the friction term in the damped harmonic oscillator equation can become a driving term, so that the decaying mode becomes a growing mode, and enhances the curvature perturbation on scales beyond the horizon. This enhancement continues until the slow-roll conditions are restored. (A similar mechanism has been used to build single field models with large squeezed non-Gaussianity [16].)

The first possible scenario that we propose is based upon an earlier observation on how subleading, non-perturbative effects can affect axion inflation [17]³. In string axion inflation, the perturbative axion shift symmetry is broken spontaneously by background vevs (*e.g.* fluxes), such as in axion monodromy [23, 24] and/or non-perturbative effects (*e.g.* string instantons), leading to large field inflation models with monomial or cosine (“natural inflation” [25]) potentials. In [17], we noted that subleading non-perturbative effects – if sufficiently large – can superimpose periodically steep cliffs and gentle plateaus onto the underlying potential. The overall effect shown there was to restore axion inflation into the favour of current CMB observations, by allowing sufficient e-folds of inflation to be obtained with smaller field ranges and thus lowering the tensor-to-scalar ratio, even achieving natural inflation with sub-Planckian axion decay constants. Here we note that such an inflationary potential can also quite naturally give rise to an enhancement in the scalar power spectrum at small scales, as the inflaton meets successively shallower plateaus on its roll towards the global minimum. Depending on the parameters, the cliffs may temporarily halt inflation, and the plateaus may include (near-)inflection points around which ultra slow-roll inflation occurs. By connecting to the heuristic arguments above, and analysing numerically the cosmological perturbations, we show that such models can both lie within 2σ constraints from Planck results, and produce a population of light PBH (about $10^{-16} - 10^{-15} M_{\odot}$) that provides a significant fraction of Dark Matter.

The second string motivated mechanism for the amplification of power during inflation that we propose is based on single field models of inflation with non-canonical kinetic terms, as for example DBI inflation [26, 27]. To understand what features are required within these models, we extend the Leach et al. argument on amplification of super-horizon

²Note however, the first toy model that can amplify the power in scalar fluctuations is proposed by Starobinsky [15].

³Other papers studying PBH production in axion inflation are [18–22], although they do not work in a single field system, since they couple the axion to gauge fields or include a spectator sector coupled to gauge fields.

modes to include varying speed of sound. We find that a driving term emerges in the mode equation if the speed of sound increases sufficiently fast. A simple way to achieve this is if the warp factor experienced by the D-brane sourcing inflation features a sufficiently large⁴ and steep step during the inflationary trajectory. A large step in the warp factor could occur for instance, if the D-brane travels down a throat within a throat, sourced by two separated stacks of D-branes [31, 32].

Another scenario could be that during the D-brane’s journey down the throat, an instability towards brane-antibrane or flux-antibrane [33] annihilation occurs at the tip of the throat. In this scenario, observations of a population of PBHs would reveal interesting properties of branes exploring the geometry of the string compactification.

The paper is organised as follows. In the following section, we provide a brief review of the basic physical mechanism which leads to the enhancement of the amplitude of curvature perturbation during inflation, subsequently leading to the production of PBHs. In Section 3, we review and develop models of string axion inflation including subleading non-perturbative effects, describing their background evolution and predictions at the CMB scales. We then investigate numerically the amplification of scalar power spectrum at small scales. In particular, we provide two explicit models which both concord with CMB observations and produce PBHs sufficient to explain a significant fraction of Dark Matter. In Section 4, we turn our attention to DBI models of inflation with a large step feature in the warp factor. We study the background evolution and the equation governing the curvature perturbations, and thus provide heuristic arguments for the amplification of curvature perturbations, postponing a detailed numerical analysis of the perturbations to future work. Finally, in Section 5 we present our conclusions and point towards several open questions to which our work leads.

We will use natural units, $\hbar = c = 1$, with reduced Planck mass $M_{\text{pl}}^2 = (8\pi G)^{-1}$. Our metric signature is mostly plus $(-, +, +, +)$. The background metric is a FRW universe with line element $ds^2 = -dt^2 + a^2(t) d\vec{x}^2 = a^2(\tau) (-d\tau^2 + d\vec{x}^2)$. The overdots and primes on time dependent quantities denote derivatives with respect to coordinate time t and conformal time τ , respectively. During inflation, we take $a(\tau) = 1/(-H\tau)^{1+\epsilon}$ with H is the physical Hubble rate.

2 Enhancing the amplitude of curvature fluctuations in single field inflation

As discussed in the introduction, the production of PBHs from inflation requires that the spectrum of curvature fluctuations has to increase by a factor of $\sim 10^7$ in its amplitude at scales well below CMB scales. Such enhanced primordial curvature fluctuations induce large matter density fluctuations at horizon re-entry, which can collapse to form PBHs.

⁴See [28, 29] for an analysis of the effects on brane inflation of the tiny, sharp steps in the warp factor caused by quantum corrections in Seiberg duality cascades [30].

At leading order in slow-roll, the amplitude of the scalar power spectrum in single field inflation with canonical kinetic terms reads

$$\Delta_s^2 = \frac{1}{4\pi^2} \frac{H^4}{|\dot{\phi}|^2} \Big|_{k=aH}, \quad (2.1)$$

where H is the Hubble parameter, and $\dot{\phi}$ denotes the time derivative of the inflaton. Deviations from a slow-roll regime can change this expression, but at first sight it seems hard to increase its value by several orders of magnitude within a well-defined range of scales, without spoiling inflation. On the other hand, various recent works have succeeded in doing so [7], by using inflationary potentials with inflection points. In the inflection point regions of the potential the inflaton dynamics experiences a rapid speed decrease, and enters into a so-called ultra slow-roll regime during which the amplitude of Δ_s^2 can indeed be enhanced by several orders of magnitude.

A heuristic, physically transparent explanation for this phenomenon can be found in works by Leach and Liddle [13] and Leach et al. [14]. We review their argument here, using it as guideline for the discussion we develop in the remaining sections.

The mode equation for curvature fluctuations of wavenumber k in single field inflation reads

$$\mathcal{R}_k'' + 2\frac{z'}{z}\mathcal{R}_k' + k^2\mathcal{R}_k = 0, \quad (2.2)$$

where the ‘‘pump field’’ for the curvature perturbation defined as $z \equiv a\dot{\phi}/H$ satisfies:

$$\frac{z'}{z} = aH(1 + \epsilon - \delta). \quad (2.3)$$

In this expression, the standard slow-roll parameters ϵ and δ are defined as

$$\epsilon \equiv -\frac{\dot{H}}{H^2}, \quad (2.4)$$

$$\delta \equiv -\frac{\ddot{H}}{2H\dot{H}} = -\frac{\dot{\epsilon}}{2\epsilon H} + \epsilon. \quad (2.5)$$

At a given moment of time during inflation, $\epsilon < 1$, while δ can be in principle of any size. Notice that the mode equation in (2.2) is of the form of a damped harmonic oscillator. In the standard slow-roll limit $\epsilon, \delta \ll 1$, we focus on modes \mathcal{R}_k which already left the horizon (*i.e.* $k < |z'/z|$).

The solution to equation (2.2) can then be expressed as

$$\mathcal{R}_k(\tau) = \mathcal{C}_1 + \mathcal{C}_2 \int \frac{d\tau}{z^2} \quad (2.6)$$

where \mathcal{C}_1 and \mathcal{C}_2 are two integration constants, multiplying respectively the constant and

decaying solutions to the equation (2.2). Since equation (2.3) implies

$$z(a) = z_0 \exp \left[\int (1 + \epsilon - \delta) d \ln a \right] \quad (2.7)$$

with z_0 a constant, we learn that $z \sim a$ in the limit where the slow-roll parameters ϵ and δ can be neglected. Since in such limit $a \sim -1/(H\tau)$, the decaying mode proportional to \mathcal{C}_2 rapidly decays as a^{-3} outside the horizon, and the curvature perturbation is then conserved at super-horizon scales, being controlled by the constant mode \mathcal{C}_1 . After matching with the Bunch-Davies vacuum at sub-horizon scales, one obtains the power spectrum amplitude of eq. (2.1) at leading order in a slow-roll approximation.

Departure from the slow-roll regime suggests a way to enhance the amplitude of curvature perturbations for modes at certain scales, right after they cross the horizon. Suppose that the friction term proportional to z'/z in (2.2) transiently *changes sign* for some short interval during the inflationary homogeneous evolution:

$$1 + \epsilon - \delta < 0. \quad (2.8)$$

In this case, the friction becomes a driving term in the equation (2.2): the exponent in eq (2.7) becomes negative, hence z decreases with time instead of increasing, implying that the mode proportional to \mathcal{C}_2 appearing in eq (2.6) is growing in this regime. Its contribution to the curvature perturbation can become substantial, increasing the size of \mathcal{R} . The once-decaying, now-growing mode \mathcal{C}_2 can thus be exploited to enhance the power spectrum of curvature fluctuations during a short range of scales [14]. Since ϵ is positive and at most order one, the condition (2.8) requires δ to be at least order one, implying that this can occur through a transition to fast-roll (where $\delta = 1$), during which the slow-roll approximation breaks down. In particular, the ultra slow-roll regime mentioned above (and that we shall discuss more at length later on) corresponds to a phase during which $\delta \geq 3$.

This is the basic physical mechanism we intend to exploit to enhance the power spectrum at small scales, and thus produce PBHs. We will apply and generalise it to two string motivated scenarios for single field inflation, the first being based on axion inflation, the second D-brane inflation with non-canonical kinetic terms.

3 PBHs in axion inflation with subleading non-perturbative effects

In this section we analyse in full detail a string motivated model for axion inflation, which includes next-to-leading, non-perturbative contributions to a monomial potential. We proceed as follows

- We start by presenting the theoretical motivations underlying this system. We show how subleading, non-perturbative corrections to the axion potential can qualitatively alter the homogeneous dynamics of the inflaton field, and work out the corresponding time evolution of the slow-roll parameters (Sections 3.1-3.3).
- We continue in Sections 3.4-3.5 by numerically studying the dynamics of curvature fluctuations in two concrete models based on this set-up, showing that they can be in good agreement with CMB measurements (typically predicting a large value for the running parameter α_s), and at the same time produce an enhancement of the curvature power spectrum at small scales, exploiting the argument of Section 2.
- In Section 3.6 we then show that our models produce a monochromatic population of light PBHs that can provide a considerable fraction of Dark Matter density. We discuss observational constraints on our PBH features, and further constraints that the production mechanism imposes on the cosmological evolution after inflation ends.

3.1 Bumpy inflation

We consider a scenario that is based upon an earlier observation on how subleading, non-perturbative effects can alter axion inflation [17]. In string axion inflation, the perturbative axion shift symmetry is broken spontaneously by background vevs (*e.g.* fluxes) or non-perturbative effects (*e.g.* string instantons), leading to large field inflation models with monomial or cosine (“natural inflation”) potentials. In [17], we noted that subleading non-perturbative corrections – if sufficiently large – can superimpose oscillations onto the underlying potential. The size of these effects will depend on the vev’s of fluxes and other moduli, which are already stabilised. Therefore, they may be tiny, large enough to introduce new local minima and maxima that may halt inflation, or anything in between. We focus on an intermediate situation, where step-like features are induced in the potential, with steep cliffs and gentle plateaus, which transiently induce large deviations from the slow-roll attractor regime.

For concreteness, we consider a string-inspired model with axion, ϕ , with a canonical kinetic term and minimal coupling to gravity:

$$\frac{\mathcal{L}}{\sqrt{-g}} = \frac{M_{\text{pl}}^2}{2} R - \frac{1}{2} \partial_\mu \phi \partial^\mu \phi - V(\phi), \quad (3.1)$$

where the axion potential takes the following form

$$V(\phi) = V_0 + \frac{1}{2} m^2 \phi^2 + \Lambda_1^4 \frac{\phi}{f} \cos\left(\frac{\phi}{f}\right) + \Lambda_2^4 \sin\left(\frac{\phi}{f}\right). \quad (3.2)$$

This class of potentials is known to arise from string theory constructions [34–37]⁵.

⁵For example, the potential of the form above arises for an axion $\text{Im}(Z)$ - after having fixed the saxion

The background dynamics of the inflaton depends on the size of the non-perturbative corrections compared to the mass term in the potential (3.2), in particular on the ratios $\beta_i \equiv \Lambda_i^4/m^2 f^2$. In the limit $\beta_i \rightarrow 0$ ($i = 1, 2$), non-perturbative corrections become negligible and we recover the usual smooth quadratic potential. For $\beta_i > 1$, one introduces a large number of new stationary points (where $V' = 0$) into the smooth ϕ^2 potential in a given range of field values. In this case, the classically rolling scalar field might eventually get stuck into some local minimum depending on the initial conditions [38]. In this work, we focus on the parameter space where $\beta_i < 1$ for both $i = 1, 2$, but without assuming $\beta_i \ll 1$.

To illustrate the general shape of the potential we are interested in, in Figure 1 we plot $V(\phi)$ in (3.2) and its slope for the parameters

$$\beta_1 \simeq 0.86, \quad \beta_2 \simeq 0.25, \quad M_{\text{pl}}/f = 1.6, \quad (\text{Case 1}) \quad (3.3)$$

while V_0 is chosen to ensure that the potential is vanishing at the minimum. The non-perturbative corrections, being subleading but considerable, introduce plateau-like regions connected by steep cliffs. Notice that the slope of the potential, V' , is positive for a large range of ϕ values but gradually decreases until it eventually vanishes at a shallow local minimum when $\phi \sim 1.35M_{\text{pl}}$. One can expect the dynamics to be such that an initially displaced ϕ rolls down in its wiggly potential, passing through the local minimum, and eventually settling on its global minimum at $\phi = 0$ [17]. In the upcoming sections, we will elaborate on the interesting dynamics that arises due to the presence of a shallow local minimum, shortly before the global minimum.

3.2 Background evolution – slow roll, fast roll

We now study the inflationary dynamics that arises from the Lagrangian (3.1) and (3.2) on a flat FRW background. Using the number of e-folds, $N(t) = \ln a(t)$, as the time variable, the system is governed by the following set of equations:

$$H^2 = \frac{V(\phi)}{M_{\text{pl}}^2(3 - \epsilon)},$$

$$\frac{d^2\phi}{dN^2} + (3 - \epsilon) \frac{d\phi}{dN} + \frac{1}{H^2} V'(\phi) = 0, \quad (3.4)$$

where ϵ is the standard Hubble slow-roll parameter,

$$\epsilon = -\frac{\dot{H}}{H^2} = \frac{1}{2M_{\text{pl}}^2} \left(\frac{d\phi}{dN} \right)^2. \quad (3.5)$$

$Re(Z)$ - from a Kähler potential $K = -\ln(Z + \bar{Z})$, superpotential $W = W_0 + MZ + i\Lambda e^{-bZ}$ and an uplift term, motivated e.g. by fluxes and non-perturbative effects. The coefficients in the potential will then depend on the fluxes W_0, M, Λ , as well as the vev of the saxion.

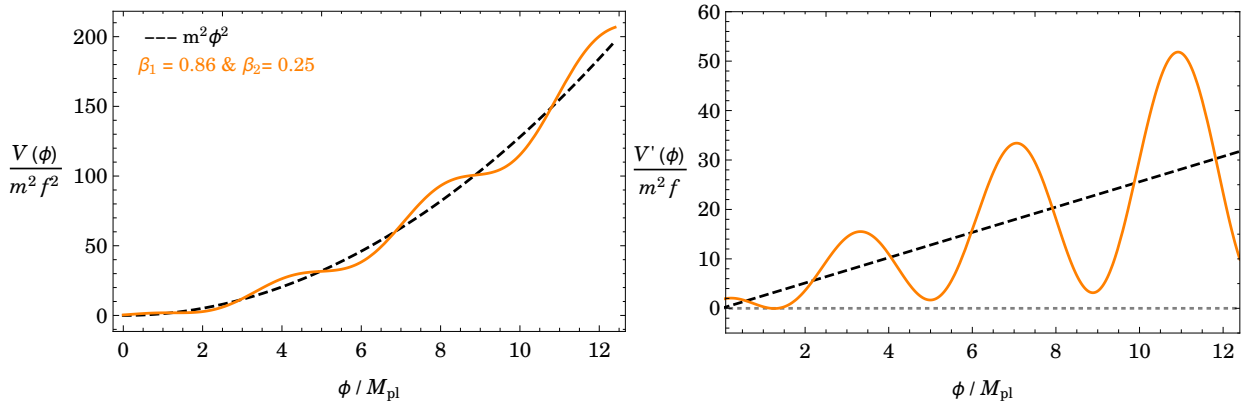


Figure 1. Potential $V(\phi)$ (left, orange) in (3.2) and its derivative $V'(\phi)$ (right, orange) for parameters $\beta_1 \equiv \Lambda_1^4/m^2 f^2 = 0.86$, $\beta_2 \equiv \Lambda_2^4/m^2 f^2 = 0.25$ and $M_{\text{pl}}/f = 1.6$, in comparison to the case of smooth quadratic potential $V_{sm}(\phi) \propto \phi^2$ (black, dashed). The gray dotted line on the right plot is shown to guide the eye towards $V'(\phi) = 0$.

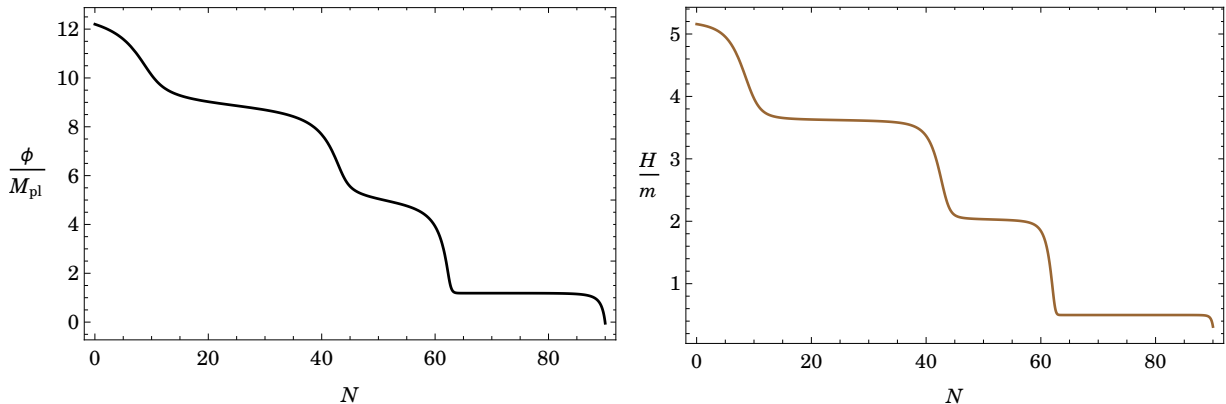


Figure 2. Background solution $\phi(N)$ (left) and $H(N)/m$ (right) in the bumpy potential (3.2) with the initial condition $\phi(0) = 12.2 M_{\text{pl}}$ where β_1 , β_2 and M_{pl}/f are taken to be the same as in Figure 1.

We numerically solve the set of equations (3.4) and (3.5) assuming initially we are in the slow-roll attractor regime, defined by the condition

$$\frac{d\phi}{dN} = -\frac{V'(\phi)}{V(\phi)}. \quad (3.6)$$

In this way, we set all the initial conditions required to solve the system only using a given initial ϕ value. As an example, we set $\phi(N_{\text{in}} = 0) = 12.2 M_{\text{pl}}$, and plot the solutions to (3.4) as a function of e-folds during inflation in Figure 2.

We find that the inflaton slowly rolls down the smooth plateau-like regions, sustaining

an almost constant Hubble friction. However, whenever it meets a cliff, the inflaton speeds up quickly, until it reaches the next plateau where Hubble friction rapidly slows it right back down again [17]. Notice also that the strength of the acceleration down the cliffs increases as the field rolls down to small field values. The system is in a slow-roll attractor regime within the plateaus, but departs from slow-roll during the acceleration and fast roll through the steeper cliffs and the during the deceleration when rolling into the flat plateaus from the steep cliffs.

This behaviour can be seen from Figure 3 where we plot the evolution of the slow-roll parameter ϵ together with the parameter:

$$\delta \equiv -\frac{\ddot{H}}{2H\dot{H}} = -\frac{\ddot{\phi}}{\dot{\phi}H}, \quad (3.7)$$

with respect to e-folds N . We see peaks in the slow-roll parameter ϵ and oscillations in δ as ϕ accelerates ($\delta < 0$) down the steep cliffs and decelerates ($\delta > 0$) into the plateaus⁶.

Note that although ϵ increases quite considerably at around $N \approx 62$, we still have $\epsilon < 1$, hence the accelerated spacetime expansion does not terminate here. Inflation lasts until $N_{\text{tot}} \simeq 90$ e-folds⁷ where $\epsilon = 1$, and ϕ begins to settle at its global minimum.

Parameter choices for the axion potential (3.2) are also possible such that ϕ rolls down the last cliff so fast that ϵ becomes larger than unity for a short period of time – temporarily halting inflation – before it rapidly decelerates at the plateau, and resumes inflation. In Figures 6,7 and 8, we present such a model, numerically solving (3.4) with parameters

$$\beta_1 \simeq 0.9, \quad \beta_2 \simeq 0.16, \quad M_{\text{pl}}/f = 1.7, \quad (\text{Case 2}) \quad (3.8)$$

and the initial condition $\phi(0) = 11.55 M_{\text{pl}}$.

3.3 Ultra slow-roll phase

The most important feature of the bumpy potential (3.2) is the behaviour of ϕ after the last cliff and through the local minimum towards the global one. Let us discuss the Case 1 parameters in eq (3.3), as Case 2 is very similar. As shown in Figure 4, at around $N \gtrsim 62$, the inflaton starts to decelerate enormously, while the slow-roll condition, $\delta < 1$ is violated for about $\Delta N \approx 4$ e-folds during which δ reaches a maximum value of⁸ $\delta \gtrsim 3$. During the time where $\delta > 1$, the friction term in the Klein-Gordon (KG) equation is not balanced by the slope of the potential as in the standard slow-roll attractor case but

⁶Note that in our conventions, the field rolls down from large to small values: this implies that the velocity is $\dot{\phi} < 0$, and acceleration corresponds to $\ddot{\phi} < 0$. Hence acceleration (deceleration) of the inflaton corresponds to the case where $\delta < 0$ ($\delta > 0$).

⁷Note that only the last ~ 65 e-folds or so of inflation have observational consequences.

⁸By definition, $\delta \equiv 3 + V'(\phi)/(\dot{\phi}H)$ using the KG equation in cosmological time. This explains why $\delta > 3$ during ultra slow-roll as $V' < 0$ around the inflection point (See *e.g.*, Figure 5).

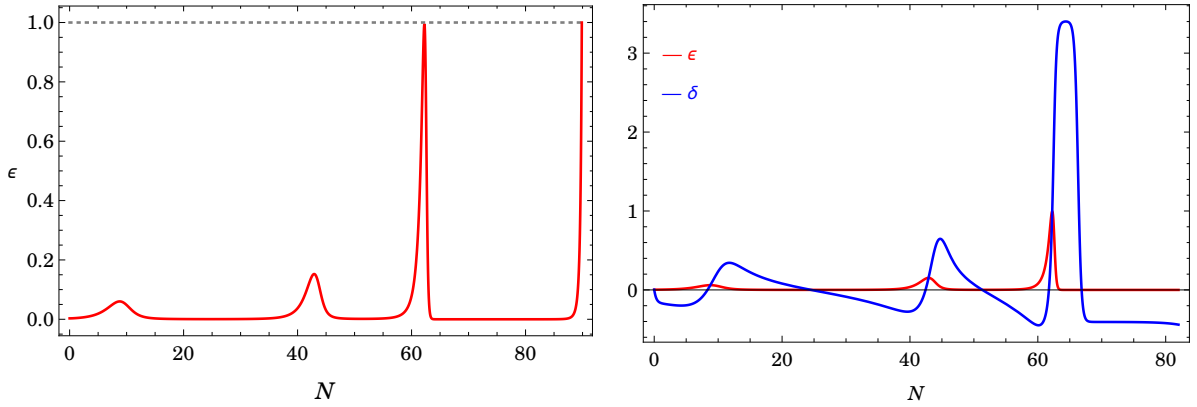


Figure 3. Evolution of the Hubble slow-roll parameters ϵ (left) and δ together with ϵ (right) as a function of e-folds N .

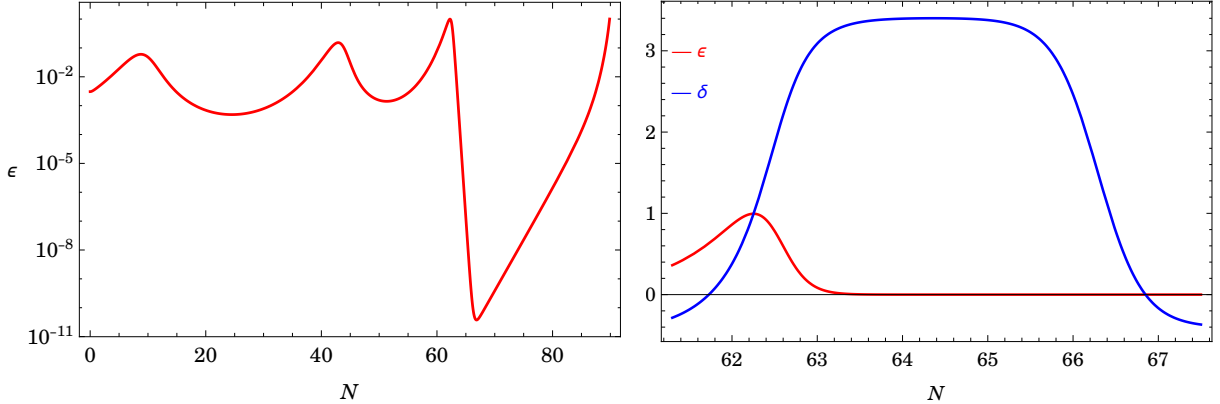


Figure 4. Evolution of ϵ in a logarithmic scale as a function of e-folds (left). Zoomed in plot for δ together with ϵ around the time where $\delta > 1$ corresponding to the evolution of the inflaton ϕ after the last cliff in the potential (3.2) (See *e.g.*, Figure 5).

with the acceleration term in (3.4), and shortly after the system enters an ‘ultra slow-roll’ regime where $\epsilon \ll 1$ and $\delta \gtrsim 3$ [39–42].

The ultra slow-roll behaviour of the inflaton can also be understood from the shape of the potential after the last cliff, shown in Figure 5: by the end of the cliff, ϕ will be rolling very fast, allowing it to overshoot the local minimum, and pass through an inflection point – shown in Figure 5 – during which it decelerates with breaks on. As the acceleration term in the Klein Gordon equation dominates over the slope of the potential in this region, the velocity of the field decreases quickly⁹, *i.e.* $\epsilon \sim e^{-(2\delta)N}$ where $\delta \gtrsim 3$ (See Figure 4). Note that although this regime is dubbed ‘ultra slow-roll’, the inflaton actually traverses the

⁹In single field inflation with canonical kinetic terms, the definition of the slow-roll parameter δ implies $d \ln \dot{\phi} = -\delta dN$. Assuming a constant δ during the ultra slow-roll regime gives $\epsilon \sim e^{-(2\delta)N}$.

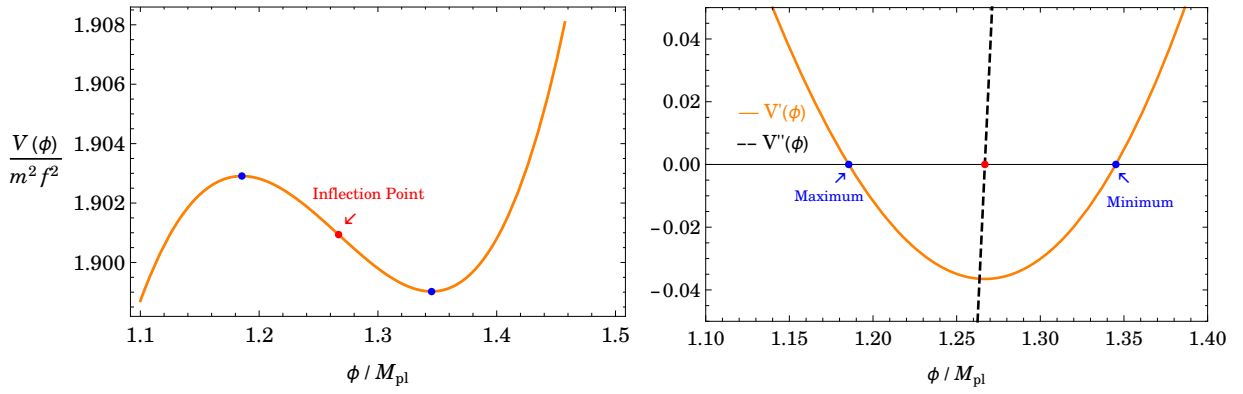


Figure 5. The shape of the potential $V(\phi)$ in (3.2) after the last cliff (left) and the behaviour of $V'(\phi)$ and $V''(\phi)$ in the same field range (right) with the same parameter choices as in Figure 1. Blue points in both graphs represents the points where $V' = 0$ whereas the red dot is an inflection point where $V'' = 0$.

relevant part of the potential very quickly (in a few e-folds) by flying over its decreasing kinetic energy. After ϕ climbs the hill shown in Figure 5, the system is back into its slow-roll attractor regime and stays in it until inflation ends.

In summary, the existence of sizeable non-perturbative corrections to the axion potential can lead to steep cliffs and gentle plateaus in the potential, including a local minimum, inflection point and maximum preceding the global minimum. We showed that in the presence of such a feature in the potential, the system enters into the ultra slow-roll regime for a few e-folds during which the slow-roll condition $\delta \ll 1$ is violated. Such an order one violation of the slow-roll condition around a (near-)inflection point can lead to an enhancement of the primordial curvature power spectrum¹⁰, in accordance with the arguments we reviewed in Section 2. We will discuss this enhancement for our model and the associated phenomenology for PBH as Dark Matter in Sections 3.5 and 3.6. Before focusing on this phenomenology at small scales, we need to make sure that the predictions of our model are in agreement with the observations at the CMB scales. This will be the topic of the following subsection.

3.4 Phenomenology at CMB scales

We have seen that during the inflationary epoch, the slow-roll parameters undergo large oscillations when the field rolls down the steep cliffs and into the plateaus of the potential (3.2). However, during the short range of e-folds that is associated with CMB scales (*e.g.* between $N = 20$ and $N = 30$ in both cases we considered), the slow-roll parameters can be small and smoothly varying [17].

¹⁰See for example [43] for a general discussion.

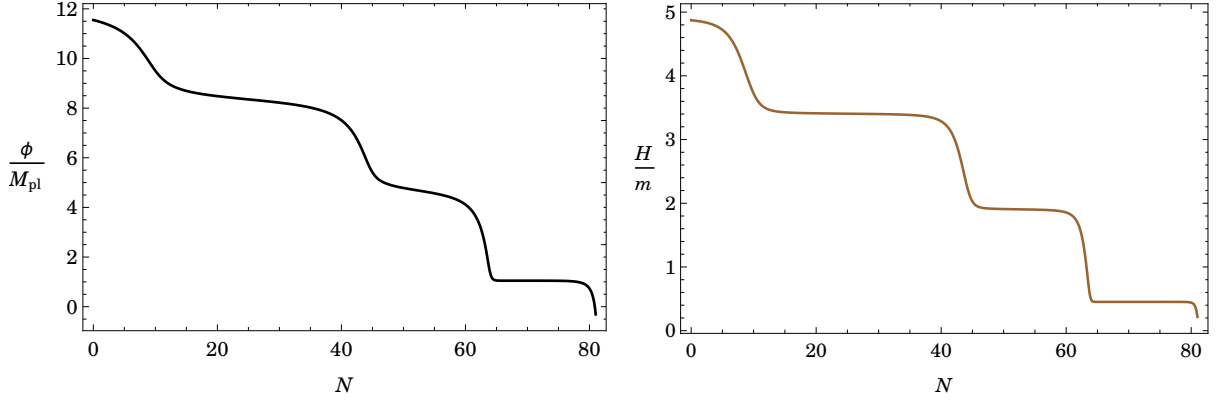


Figure 6. Background solution to $\phi(N)$ (left) and $H(N)/m$ (right) in the bumpy potential (3.2) with the initial condition $\phi(0) = 11.55 M_{\text{pl}}$ where $\beta_1 \simeq 0.9$, $\beta_2 \simeq 0.16$ and $M_{\text{pl}}/f = 1.7$.

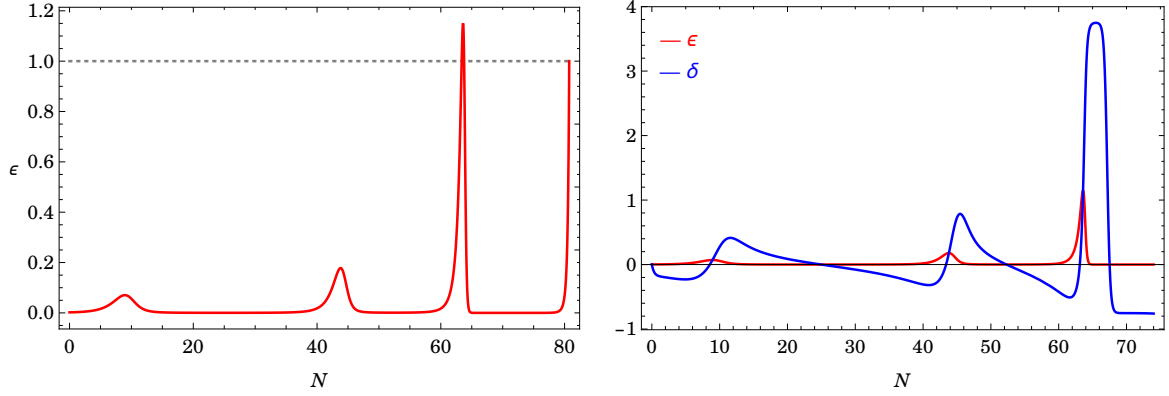


Figure 7. Evolution of the Hubble slow-roll parameters ϵ (left) and δ together with ϵ (right) as a function of e-folds N for the parameter choices as in Figure 6.

We first estimate the CMB observables using the slow-roll approximation. For this purpose, we define the slow-roll parameters as

$$\epsilon = -\frac{\dot{H}}{H^2}, \quad \delta = -\frac{\ddot{H}}{2H\dot{H}}, \quad \xi^2 = \frac{\ddot{H}\dot{H} - \ddot{H}^2}{2\dot{H}^2 H^2}, \quad \sigma^3 = \frac{7\dot{H}\ddot{H}\ddot{H} - 2\dot{H}^2\ddot{H} - 5\ddot{H}^3}{4\dot{H}^3 H^3}. \quad (3.9)$$

In terms of these slow-roll parameters, the key observables describing the power spectrum of scalar and tensor perturbations are given by [44–46],

$$\Delta_s^2 = [1 + (2 - \ln 2 - \gamma)(2\epsilon + \delta) - \epsilon]^2 \frac{H^2}{8\pi^2 \epsilon M_{\text{pl}}^2},$$

$$\Delta_t^2 = [1 - (\ln 2 + \gamma - 1)\epsilon]^2 \frac{2}{\pi^2} \frac{H^2}{M_{\text{pl}}^2}, \quad r = \frac{\Delta_t^2}{\Delta_s^2},$$

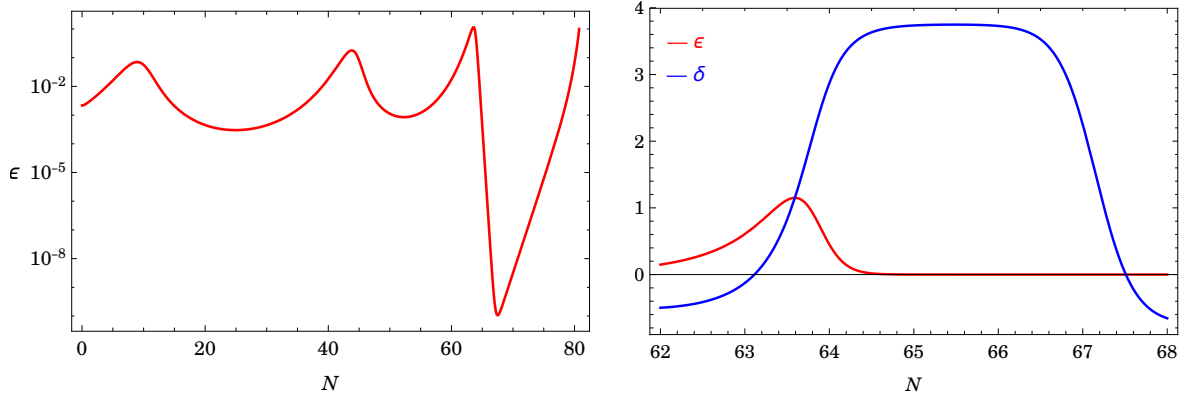


Figure 8. Evolution of ϵ in a logarithmic scale as a function of e-folds (left). Zoomed in plot for δ together with ϵ .

$$\begin{aligned}
n_s &= 1 - 4\epsilon + 2\delta - 2(1 + \mathcal{C})\epsilon^2 - \frac{1}{2}(3 - 5\mathcal{C})\epsilon\delta + \frac{1}{2}(3 - \mathcal{C})\xi^2, \\
\alpha_s &= -2\xi^2 + 10\epsilon\delta - 8\epsilon^2, \\
\beta_s &= -32\epsilon^3 + 62\epsilon^2\delta - 20\epsilon\delta^2 + 2\sigma^3 - 14\epsilon\xi^2 + 2\delta\xi^2,
\end{aligned}
\tag{3.10}$$

where γ is the Euler-Mascheroni constant and $\mathcal{C} \equiv 4(\ln 2 + \gamma) - 5$. All time dependent quantities in the expressions above should be evaluated at the time of horizon crossing¹¹ N_{hc} where the comoving pivot scale $k = k_*$ leaves the horizon $(a_{\text{hc}}H_{\text{hc}})^{-1}$. To determine the time of horizon crossing, we first use the numerical solutions to the FRW background equations (3.4) to describe the evolution of the Hubble slow-roll parameters in (3.9) in terms of the number of e-folds N and then impose the following measurements and bounds on the CMB observables from¹² Planck 2015 (at $k_* = 0.05 \text{ Mpc}^{-1}$ and 68% CL for TT+lowP+BAO) [47],

$$\begin{aligned}
\ln(10^{10}A_s) &= 3.093 \pm 0.034, \\
n_s &= 0.9673 \pm 0.0043, \\
\alpha_s &= -0.0125 \pm 0.0091, \\
r &< 0.166 \quad (\text{the Planck/KEK combined analysis gives } r < 0.07),
\end{aligned}
\tag{3.11}$$

where A_s is the amplitude of the curvature power spectrum.

In practice, we use the expression for scalar tilt in (3.10) and impose the central value,

¹¹In single field inflation, we can always invert $\phi(N)$ to describe the slow-roll parameters in (3.9) as a function of e-folds N .

¹²In the bumpy model we are investigating, the running of the running, β_s , is suppressed two orders of magnitude below α_s . Therefore we will not consider the Planck results including β_s .

	Case 1: $M_{\text{pl}}/f = 1.6$	Case 2: $M_{\text{pl}}/f = 1.7$
N_*	63.593	54.015
$V_0^{1/4}$	9.98285×10^{-4}	8.64799×10^{-4}
m	$2.563395477 \times 10^{-6}$	$2.12915358 \times 10^{-6}$
Λ_1	1.218164×10^{-3}	$1.08856568 \times 10^{-3}$
Λ_2	8.9630812×10^{-4}	7.1318712×10^{-4}

Table 1. N_* and the relevant mass scales in units of M_{pl} in the axion potential (3.2).

Observables	Case 1: $M_{\text{pl}}/f = 1.6$	Case 2: $M_{\text{pl}}/f = 1.7$
n_s	0.96717	0.96408
α_s	-0.03056	-0.02987
β_s	2.78×10^{-4}	1.44×10^{-4}
r	7.88×10^{-3}	4.83×10^{-3}
n_t	-1.08×10^{-3}	-6.43×10^{-4}

Table 2. Observables in bumpy axion inflation evaluated at the pivot scale $k_* = 0.05 \text{ Mpc}^{-1}$.

$n_s = 0.9673$ to obtain the e-folding number at which the pivot scale crosses the horizon, N_{hc} . This allows us to determine the number of e-folds before the end of inflation at which the pivot scale crosses the horizon, *i.e.* $N_* \equiv N_{\text{tot}} - N_{\text{hc}}$. On the other hand, notice that in the previous section, we have scaled out the mass m of the inflaton from all of our equations when we solve for the background evolution. Using the normalization of the power spectrum, $\Delta_s^2 = 2.2 \times 10^{-9}$, we fix the mass scale m which in turn allows us to determine Λ_i from a given β_i . We list in Table 1 the values of N_* and the parameters that we use in the axion potential (3.2).

Calculating the observables by evaluating the expressions in (3.10) at horizon crossing could lead to inaccurate results as the slow-roll parameter δ evolves considerably around this time (see Figures 3, 7) [14]. Therefore, to obtain reliable results, we have used the code¹³ `MultiModeCode` [48–53]. This program is optimized for multi-field inflation, but its detailed implementation makes it easy to evolve single field background and perturbation equations at the linearized level with the bumpy potential defined in (3.2). Using the parameter sets given in Table 1, we summarize the output of the program for the key observables in Table 2. We see that all the observables associated with scalar fluctuations agree with the 2σ (95% CL) limits of the Planck data (see *e.g.* (3.11)). The reason behind the large negative running can also be understood by evaluating the slow-roll parameters (3.9) at horizon crossing:

¹³Web page: www.modecode.org

$$\begin{aligned}
\text{Case 1 : } \quad & \epsilon \approx 5 \times 10^{-4}, \quad \delta \approx -0.013, \quad \xi^2 \approx 0.004, \\
\text{Case 2 : } \quad & \epsilon \approx 3 \times 10^{-4}, \quad \delta \approx -0.027, \quad \xi^2 \approx 0.015 \quad .
\end{aligned}
\tag{3.12}$$

Notice that although the first slow-roll parameter ϵ is small, a large δ and ξ^2 leads to a large running α_s of the spectral index n_s . However, such large negative values of the running α_s are still within 2σ limits of the Planck data (3.11). Large values for the parameter α_s is a generic prediction of our system based on a potential with wiggles [17, 54].

For the two cases discussed in this section, the field excursion during the observable range of inflation is $\Delta\phi > M_{\text{pl}}$. In particular, in Case 1 we found that $\Delta\phi \simeq 8.7M_{\text{pl}}$ whereas in Case 2, where inflation stops for a short time, $\Delta\phi \simeq 8.1M_{\text{pl}}$. Thus we have a smaller field range as compared to the smooth quadratic potential, which requires $\Delta\phi \simeq 15M_{\text{pl}}$. The scale of inflation, $E_{\text{inf}} \equiv (3H_*^2 M_{\text{pl}}^2)^{1/4}$, on the other hand, is given by

$$\text{Case 1 : } \quad E_{\text{inf}} \simeq 4 \times 10^{-3} M_{\text{pl}}, \quad \text{Case 2 : } \quad E_{\text{inf}} \simeq 3.5 \times 10^{-3} M_{\text{pl}}.
\tag{3.13}$$

In the light of these results, it is interesting to note that the presence of sizeable non-perturbative corrections in the potential (3.2) can give rise to a large field realization of axion inflation where a tensor-to-scalar ratio $r \approx 10^{-2} - 10^{-3}$ can be obtained. In particular, we emphasize that although such values for the tensor-to-scalar ratio r are typically small in comparison to the smooth monomial type potential ϕ^2 [17], they are within the sensitivity of next stage CMB experiments [55].

3.5 Amplification of curvature perturbations at small scales

In Section 3.3, we have seen that the background evolution of the inflaton in the bumpy potential (3.2) can give rise to an ultra slow-roll era at small field values compared to the ones associated with the CMB. As we have emphasized before, this ultra slow-roll phase corresponds to a violation of slow-roll condition, where $\epsilon \ll 1$ but $\delta > 1$. As we discussed in our initial Section 2, this regime can be characterised by an enhancement of the curvature power spectrum, thanks to the contribution of the would-be decaying mode that is actually growing when the combination $z'/z = aH(1 + \epsilon - \delta)$ is negative.

Both of the examples we presented in Section 3.2 – in eqs (3.3) and (3.8) – fit well with the argument developed in Section 2, during the phases where the system first enters a fast-roll regime ($\delta = 1$), followed by an ultra slow-roll era, $\delta \gtrsim 3$. To illustrate this fact, in Figure 9, we superimpose the plot of the function $(aH)^{-1} z'/z$ with that of ϵ and δ for the two representative cases we discussed in Section 3.2 (see *e.g.* Figures 4 and 8). We observe that a turn around in $|z|$ occurs shortly after the time when $\delta > 1$ and z'/z continues to be negative into the ultra slow-roll regime where $\delta \gtrsim 3$, implying a growth in \mathcal{R}_k until the system returns back to the slow-roll phase. Notice also that the shape of the z'/z in this region is identical to the one of δ , which implies that the negativity of this function is mainly dictated by a large value of δ .

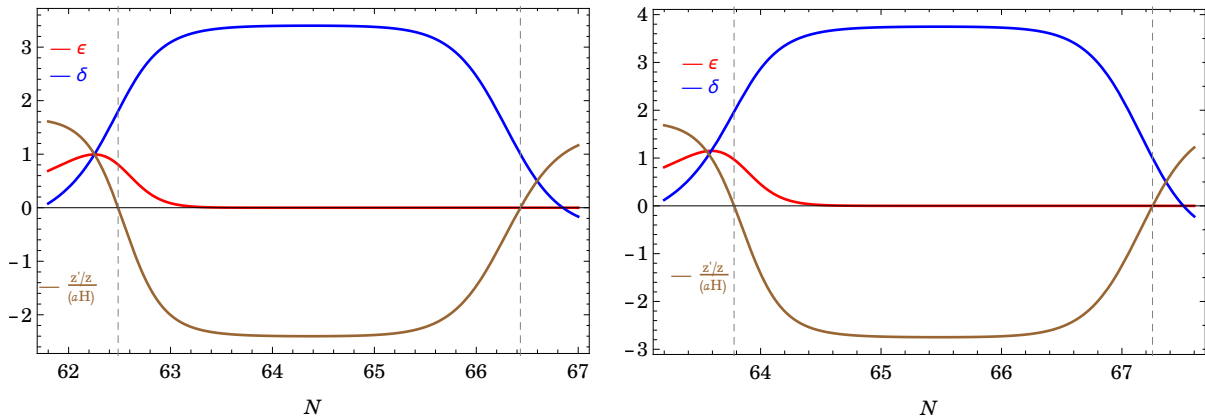


Figure 9. Evolution of the $1 + \epsilon - \delta$ as a function of e-folds around the ultra slow-roll regime for the examples we presented in Section 3.2. $z'/z < 0$ between the two vertical dashed lines.

In addition to the heuristic understanding we presented above, we also analysed numerically the full power spectrum of curvature perturbations defined by $\Delta_s^2(k) \equiv k^3 |\mathcal{R}_k|^2 / (2\pi^2)$. Given the complexity of the scalar potential and of the background dynamics we described above, we solve the linearized perturbation equations numerically using the `MultiModeCode` to obtain the full power spectrum. The resulting scalar power spectra, using the parameters provided in Table 1, is shown in Figure 10. We see that both of the scalar power spectra start to grow at comoving scales $k > 10^{13} \text{ Mpc}^{-1}$ and peak around $k \approx 7 \times 10^{13} - 10^{14} \text{ Mpc}^{-1}$, reaching a value of $\Delta_s^2 \approx 10^{-2}$. As we have explained, the reason for the growth in the power spectrum is the ultra slow-roll regime while ϕ overshoots a local minimum of the bumpy potential at Planckian field values (see *e.g.* Figure 5). In the following section, we investigate the phenomenology arising from these peaks in the power spectrum.

3.6 PBHs from non-perturbative effects in axion inflation

PBHs may have formed in the very early Universe if a sufficiently large amplitude of primordial fluctuation is generated at small scales ($k \gg k_* = 0.05 \text{ Mpc}^{-1}$) during inflation. In an inflationary Universe such a mode is stretched outside the comoving horizon and it re-enters the horizon at a later time after the end of inflation. If the amplitude of these fluctuations is significant, there will be regions in the Universe where the density of matter is so large that it can collapse to form PBHs upon horizon re-entry [1, 2]. PBHs can have observational implications at the current epoch by contributing to the present “cold” Dark Matter density if they are massive enough to avoid Hawking evaporation [56, 57].

In the simplest case, the mass of the resulting PBHs is assumed to be proportional to mass inside the Hubble volume at the time of horizon re-entry (at the time of PBH

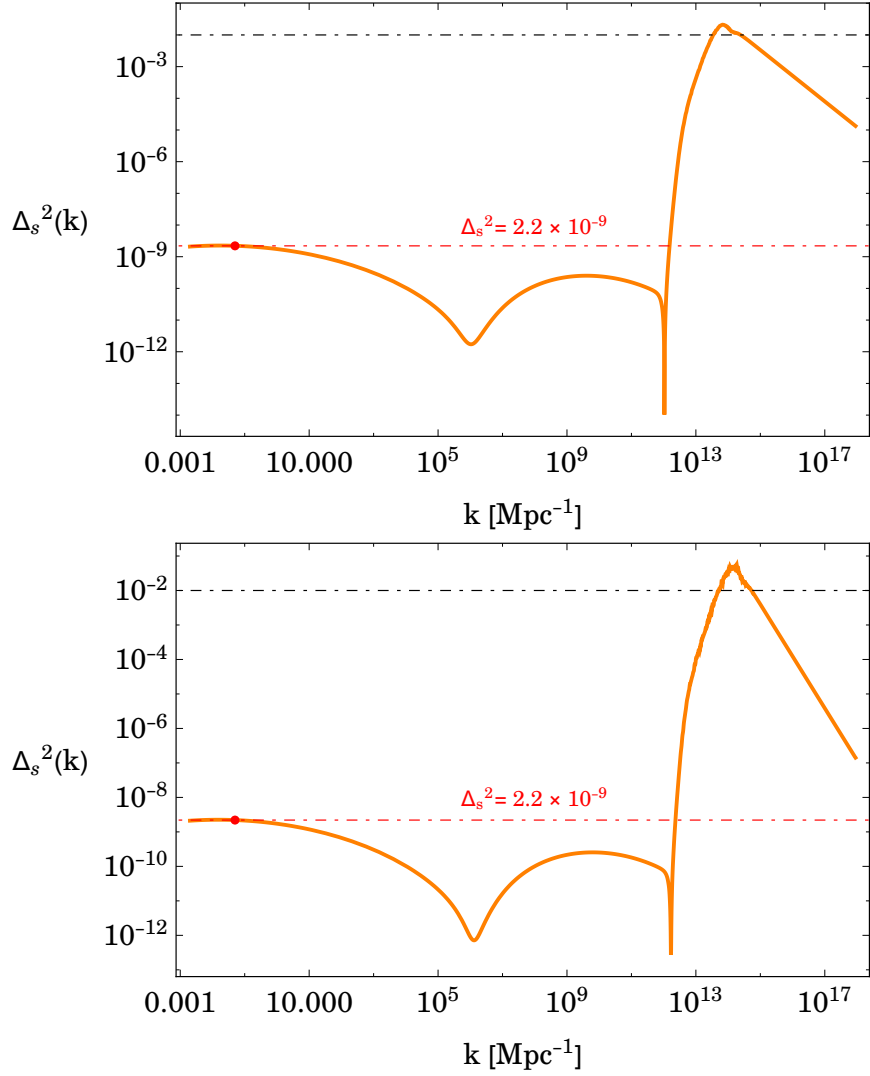


Figure 10. Power spectrum of scalar curvature perturbation in bumpy axion inflation with the parameter choices shown in Table 1 (Case 1-top panel, Case 2-bottom panel). Red dot in the graph represent the point where $\Delta_s^2 = 2.2 \times 10^{-9}$ and $k_* = 0.05$ Mpc $^{-1}$.

formation) of a mode with wavenumber k :

$$M(k) = \gamma \frac{4\pi}{3} \rho H^{-3} \Big|_{k=a_f H_f} = \gamma M_{\text{eq}}^{\text{H}} \left(\frac{\rho_f}{\rho_{\text{eq}}} \right)^{1/2} \frac{H_{\text{eq}}^2}{H_f^2} \quad (3.14)$$

where M_{eq}^{H} is the horizon mass at the time of matter-radiation equality and the subscripts “ f ” and “ eq ” denote quantities evaluated at the time of PBH formation and matter-radiation equality, respectively. Using the conservation of entropy, $g_s(T) T^3 a^3 = \text{const.}$ and the scaling of the energy density with the temperature in the radiation dominated

era, $\rho \propto g_*(T) T^4$, the mass of the PBHs can be expressed in terms of the comoving wavenumber k as

$$M(k) = \gamma M_{\text{eq}}^{\text{H}} \left(\frac{g_*(T_f)}{g_*(T_{\text{eq}})} \right)^{1/2} \left(\frac{g_s(T_{\text{eq}})}{g_s(T_f)} \right)^{2/3} \left(\frac{k_{\text{eq}}}{k} \right)^2 \\ \simeq 1.6 \times 10^{18} \text{ g} \left(\frac{\gamma}{0.2} \right) \left(\frac{g_*(T_f)}{106.75} \right)^{-1/6} \left(\frac{k}{5.5 \times 10^{13} \text{ Mpc}^{-1}} \right)^{-2}, \quad (3.15)$$

where in the second line we assumed $g_*(T) = g_s(T)$ and used $M_{\text{eq}}^{\text{H}} \simeq 5.6 \times 10^{50} \text{ g}$ [58], $g_*(T_{\text{eq}}) = 3.38$, $k_{\text{eq}} = 0.07 \Omega_m h^2 \text{ Mpc}^{-1}$. The value of the constant of proportionality $\gamma = 0.2$ is suggested by the analytical model in [56] for PBHs formed during the radiation dominated era.

The standard treatment of PBH formation is based on the Press-Schechter model of the gravitational collapse that is used widely in large-scale structure studies [59]. In this context, the energy density fraction in PBHs of mass M at the time of formation, which is denoted by $\beta(M)$, is given by the probability that the fractional overdensity $\delta \equiv \delta\rho/\rho$ is above a certain threshold δ_c for PBH formation. For Gaussian primordial fluctuations¹⁴, $\beta(M)$ is given by

$$\beta(M(k)) \equiv \frac{\rho_{\text{PBH}}}{\rho} = 2 \int_{\delta_c}^{\infty} \frac{d\delta}{\sqrt{2\pi}\sigma(M(k))} \exp\left(-\frac{\delta^2}{2\sigma^2(M(k))}\right), \\ = \sqrt{\frac{2}{\pi}} \frac{\sigma(M(k))}{\delta_c} \exp\left(-\frac{\delta_c^2}{2\sigma^2(M(k))}\right) \quad (3.16)$$

where the factor of 2 accounts for locally under threshold regions collapsing in globally over threshold regions and we have assumed $\delta_c > \sigma$ in the second line of (3.16). The value of the $\beta(M)$ is uniquely determined by the variance $\sigma^2(M(k))$ which is assumed to be coarse-grained variance smoothed on a scale of $R = k^{-1}$. During the radiation dominated era, it is given by the following expression [70],

$$\sigma^2(M(k)) = \frac{16}{81} \int_0^{\infty} d \ln q \left(\frac{q}{k} \right)^4 \Delta_s^2(q) W(q/k)^2, \quad (3.17)$$

where Δ_s^2 is the power spectrum of curvature perturbation and $W(x)$ is a smoothing window function which is usually taken to be of the Gaussian form, $W(x) = \exp(-x^2/2)$.

¹⁴The presence of local non-Gaussianity can significantly alter the PBH abundance [60–65]. Although non-Gaussianities at CMB scales for our model are small ($|f_{\text{NL}}| \sim 10^{-4}$ at $k_* = 0.05 \text{ Mpc}^{-1}$), consistently with Maldacena’s consistency relation for single-field slow-roll models [66], non-Gaussianities during the ultra slow-roll regime at small scales may be sizeable [67]. However, if the transition between ultra slow-roll and slow-roll is smooth, as is the case here, then those non-Gaussianities are washed out by subsequent evolution [68], and thus we can neglect the effects of non-Gaussianities when calculating PBH abundances. See also [69] for a discussion on the vanishing of observable primordial local non-Gaussianity in canonical single-field inflation.

At the time of their formation, a fraction, $\gamma\beta(M(k))\rho|_{k=a_f H_f}$, of the total energy in the Universe turns into PBHs. After their formation, β grows inversely proportional to the cosmic temperature ($\propto a$) until matter-radiation equality, since PBHs essentially behave as pressureless dust ($\rho_{\text{PBH}} \propto a^{-3}$). Therefore, the fraction of PBH abundance in Dark Matter today can be determined by a simple red-shifting relation [71]

$$\begin{aligned} \frac{\Omega_{\text{PBH}}(M(k))}{\Omega_{\text{DM}}} &= \left(\frac{T_f}{T_{\text{eq}}} \frac{\Omega_m}{\Omega_{\text{DM}}} \right) \gamma\beta(M(k)), \\ &\simeq \left(\frac{\beta(M(k))}{10^{-15}} \right) \left(\frac{\gamma}{0.2} \right)^{3/2} \left(\frac{g_*(T_f)}{106.75} \right)^{-1/4} \left(\frac{M(k)}{1.6 \times 10^{18} \text{ g}} \right)^{-1/2}, \end{aligned} \quad (3.18)$$

where T_f is the temperature of the plasma at the time of PBH formation and T_{eq} is the temperature at matter-radiation equality. In order to determine the ratio of the total energy density in PBHs today to that of Dark Matter, we integrate over all masses M ,

$$\frac{\Omega_{\text{PBH}}^{\text{tot}}}{\Omega_{\text{DM}}} = \int d \ln(M(k)) \frac{\Omega_{\text{PBH}}(M(k))}{\Omega_{\text{DM}}}. \quad (3.19)$$

It is clear from the expression in (3.18) that PBHs of mass $M \sim 10^{18}$ g can constitute a significant fraction of Dark Matter density today if $\beta(M)$ is within a couple of orders of magnitude of $\sim 10^{-15}$. On the other hand, it is worth emphasizing that the PBH abundance is exponentially sensitive to the critical threshold density for collapse δ_c and the variance σ^2 (see equation (3.16)). In the following, to estimate the total PBH abundance with respect to Dark Matter abundance today, we will take values of δ_c within the range $\delta_c = 0.3 - 0.5$ as suggested in [56, 72, 73]. For these values of δ_c , one requires $\sigma^2(M) \sim 10^{-2} - 10^{-3}$ to reach the required level $\beta(M)$ on the relevant scale k (or M). This in turn arises from a power spectrum in equation (3.17) that is also of the order of 10^{-2} .

Figure 10 shows that both examples we presented in the previous sections satisfy this criterion where both power spectra have sharp peaks around $k \sim 5 \times 10^{13} - 10^{14} \text{ Mpc}^{-1}$. To illustrate this further, we calculate $\beta(k)$ in (3.16) by numerically integrating the variance in (3.17) using the full power spectrum $\Delta_s^2(q)$. The resulting $\beta(k)$ for a range of comoving wave numbers including its peak is shown in Figure 11. Only the range of k values shown in this plot have a significant contribution to the total PBH abundance which can be calculated numerically using the fact that $\Omega_{\text{PBH}}/\Omega_{\text{DM}} \propto \int dk \beta(k)$. In Table 3, we summarize these results on the fraction of PBHs in Dark Matter today and the peak value for the mass of PBHs (using (3.14) with $M_{\text{peak}} \equiv M(k = k_{\text{peak}})$) obtained from the inflationary models we considered in Table 1.

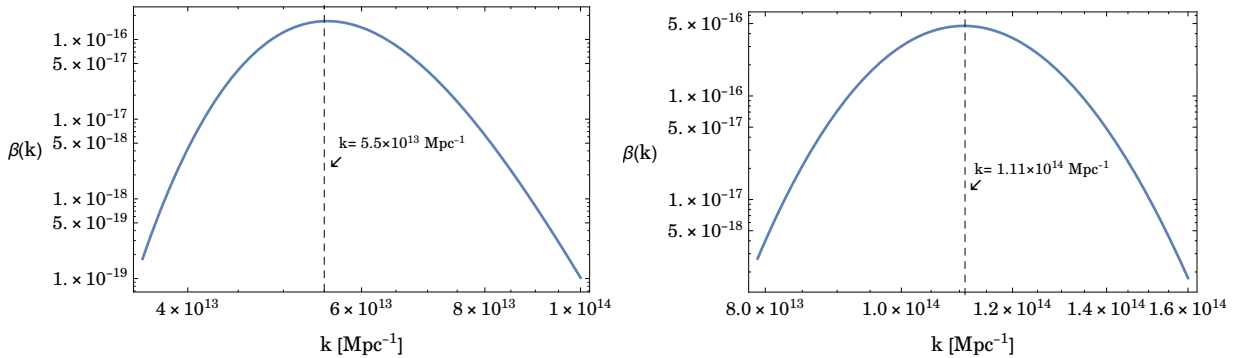


Figure 11. β as a function of the smoothing scale k . The values of k where $\beta(k)$ has a peak is also shown with dashed vertical lines.

Cases	δ_c	$M_{\text{peak}}/M_{\odot}$	$\Omega_{\text{PBH}}^{\text{tot}}/\Omega_{\text{DM}}$
$M_{\text{pl}}/f = 1.6$	0.34	8×10^{-16}	0.113
$M_{\text{pl}}/f = 1.7$	0.5	2×10^{-16}	0.514

Table 3. The two different choices of the critical threshold overdensity δ_c and the corresponding total abundance of PBHs for the models considered in Table 1. The peak value of the mass of the relevant PBHs which are obtained from the equation (3.14), is also shown.

3.6.1 Observational constraints on PBH abundance

We have seen that axion inflation with subleading non-perturbative corrections can give rise to PBHs of mass $M \simeq 3.9 \times 10^{17} - 10^{18}g$, which can constitute an $\mathcal{O}(1)$ fraction¹⁵ of Dark Matter today. It has been pointed out that such compact objects can induce features in the photon spectrum of the gamma-ray bursts that occur at cosmological distances [74]. The angular separation of these photon sources which would be lensed by such small PBHs is around the femto scale, hence the class of constraints obtained by these sources is called “femto-lensing”. Recent analysis on femto-lensing of gamma ray bursts shows that PBHs in the mass range $5 \times 10^{17} - 10^{20}g$ cannot constitute more than 10% of Dark Matter [75]. In particular, for the realization of axion inflation with the first parameter set given in Table 1, the PBH abundance cannot be much higher than the level shown in Table 3. However, the constraints¹⁶ become weaker for the smaller mass PBHs found in the case where inflation terminates for a short period of time, and thus do not exclude the interesting possibility that these tiny PBHs provide a significant fraction of Dark Matter (see *e.g.* Figure 1 of [9] or Figure 4 of [3]).

¹⁵Recall that $\Omega_{\text{PBH}}^{\text{tot}}/\Omega_{\text{DM}}$ is exponentially sensitive to the value of δ_c which can be adjusted within the suggested range in the literature to increase PBH abundance.

¹⁶Note however that constraints on the PBH fraction tend to become stronger for non-monochromatic mass functions in this range of PBH masses [76].

In summary, we have found that axion inflation with subleading but significant non-perturbative corrections is capable of generating a population of light PBHs ($M \simeq 10^{-15} - 10^{-16} M_\odot$) that might account for a considerable fraction of Dark Matter in the Universe. It is also interesting to note that there is no known astrophysical mechanism that can produce black holes with such small mass. Here we have proposed a string theory inspired primordial mechanism that can produce small mass black holes.

3.6.2 Implications for reheating

In the bumpy axion inflation we are considering here, in order to both account for a large enough amplification in the scalar power spectrum at small scales and an agreement with observations at CMB scales by Planck, the observable scales associated with the CMB had to leave the horizon at values of¹⁷ $N_* = N_{\text{tot}} - N_{\text{hc}}$ given in Table 1. In this section, we will discuss the theoretical implications of these values on the reheating phase after inflation.

In general, there is a theoretical uncertainty in determining N_* due to the unknown thermal history of the Universe after inflation. Parametrizing our ignorance about the post-inflationary Universe by an average equation of state w_p and the energy density at the time of reheating ρ_{rh} , we can quantify this uncertainty by using the matching equation [49, 77, 78],

$$N(k) = -71.21 - \frac{1}{4} \ln \left(\frac{\rho_{\text{end}}}{M_{\text{pl}}^4} \right) - \ln \left(\frac{k}{H_*} \right) + \frac{(1 - 3w_p)}{12(1 + w_p)} \ln \left(\frac{\rho_{\text{rh}}}{\rho_{\text{end}}} \right). \quad (3.20)$$

Denoting by N_*^{inst} the value of N_* in the case of instantaneous reheating, *i.e.* $\rho_{\text{rh}} \rightarrow \rho_{\text{end}}$, we can write:

$$\delta N \equiv N_* - N_*^{\text{inst}} = \frac{(1 - 3w_p)}{12(1 + w_p)} \ln \left(\frac{\rho_{\text{rh}}}{\rho_{\text{end}}} \right). \quad (3.21)$$

On the other hand, earlier in our discussion we have assumed that the PBH formation occurs during the radiation dominated era after thermalization is complete. This implies that the temperature of the plasma at the time of PBH formation is less than the temperature at the time of reheating, $T_{\text{rh}} \geq T_f$, where we can quantify T_f using the general expression in (3.14) as

$$T_f \simeq 2.65 \times 10^6 \text{ GeV} \left(\frac{\gamma}{0.2} \right)^{1/2} \left(\frac{g_*(T_f)}{106.75} \right)^{-1/4} \left(\frac{M}{8 \times 10^{-16} M_\odot} \right)^{-1/2}. \quad (3.22)$$

With the choices of parameters shown in Table 1, we numerically obtained the energy

¹⁷In fact, in order to increase the amplification of power spectrum on small scales, one is required to tune (by increasing) Λ_1 at the level shown in Table 1 which in turn increases the total number of e-folds during inflation without altering N_{hc} , implying a larger $N_* = N_{\text{tot}} - N_{\text{hc}}$.

density at the end of inflation $\rho_{\text{end}} \equiv 3/2 V_{\text{end}}$ as

$$\text{Case 1 : } \rho_{\text{end}} = 2.7 \times 10^{-12} M_{\text{pl}}^4, \quad \text{Case 2 : } \rho_{\text{end}} = 1.6 \times 10^{-12} M_{\text{pl}}^4. \quad (3.23)$$

Therefore for both cases, using the expression for T_f with the fiducial choices of parameters in (3.22), δN can be estimated as

$$\delta N \simeq \frac{(1 - 3w_p)}{12(1 + w_p)} \ln \left(10^{-35} \left(\frac{g_*(T_{\text{rh}})}{106.75} \right) \left(\frac{T_{\text{rh}}}{T_f} \right)^4 \right). \quad (3.24)$$

On the other hand, using our numerical results of Section 3.2, in the bumpy axion inflation we obtained $N_*^{\text{inst}} \simeq 57$ at $k_* = 0.05 \text{ Mpc}^{-1}$, corresponding to $\delta N \simeq 6.59$ (Case 1) and $\delta N \simeq -3$ (Case 2) by reading the values of N_* from Table 1.

Note from the equation (3.24) that to obtain a positive δN , a non-trivial average equation of state is required in the post-inflationary¹⁸ Universe, *i.e.* $1/3 < w_p < 1$ since $\rho_{\text{rh}} \leq \rho_{\text{end}}$. Assuming the smallest available value of the argument of the logarithm (*i.e.* $T_{\text{rh}} = T_f$) in (3.24), one can reach to a maximum value of $\delta N \simeq 6.7$ by an average equation of state corresponding to a stiff fluid $w_p = 1$. This implies that interesting phenomenology in the bumpy axion inflation with the parameter choices in Case 1 is only possible if a kination type of fluid [80, 81] dominates the energy density of the post-inflationary Universe until $T_{\text{rh}} \simeq 10^6 \text{ GeV}$. In the Case 2 however, theoretical requirements on the post-inflationary evolution is much less restrictive because one can easily accommodate $\delta N \simeq -3$ for a wide range of reheating temperatures T_{rh} assuming a non-standard cosmology¹⁹ with an average equation of state satisfying $0 \leq w_p < 1/3$.

4 DBI inflation with steps in the warp factor

In the previous section, we have seen that suitable choices of string inspired scalar potentials can lead to the production of PBHs, through a small scale enhancement of the curvature power spectrum induced by rapid changes in some of the slow-roll parameters. String theory also motivates models of inflation with non-standard kinetic terms, with a scalar Lagrangian expressed as

$$\mathcal{L}_\phi = \sqrt{-g} P(X, \phi) \quad (4.1)$$

where $X \equiv \frac{1}{2}(\partial\phi)^2$, and P a certain function P of X, ϕ . In this section, we begin to explore whether appropriate choices of the kinetic function P can provide the kind of violations of slow-roll conditions which enhances the scalar power spectrum, motivated by

¹⁸A non-standard post-inflationary evolution can give rise to further changes in δN as discussed in [79] for a string theory motivated scalar-tensor evolution after inflation.

¹⁹Such cosmologies could be favoured by certain string theory constructions, see for example [82] and other possible observational effects that might arise in these scenarios [83–85].

a generalization of the argument presented in Section 2. Our analysis here will be only qualitative – we do not numerically compute the power spectrum in this case – but serves as starting point for further quantitative studies of black hole production in scalar-tensor theories of single field inflation with non-standard kinetic terms.

4.1 Background and perturbations with non-canonical kinetic terms

We start by writing the homogeneous equations of motion associated with the general Lagrangian with non-canonical kinetic terms, eq (4.1), minimally coupled with Einstein gravity:

$$H^2 = \frac{8\pi G}{3}\rho, \quad (4.2)$$

$$\dot{H} = -4\pi G(\rho + P), \quad (4.3)$$

$$\dot{\rho} = -3H(\rho + P). \quad (4.4)$$

The energy density is

$$\rho = 2XP_{,X} - P, \quad (4.5)$$

while the function P in eq (4.1) plays the role of pressure. The dot indicates derivatives along physical time t . This system is characterized by a sound speed²⁰ c_s defined by

$$c_s^2 = \frac{P_X}{\rho_X} = \frac{P_X}{P_X + 2XP_{XX}}. \quad (4.6)$$

Following the formalism developed by Garriga and Mukhanov [90], the equation for the curvature perturbation \mathcal{R} generalises eq. (2.2) and reads in this case

$$\mathcal{R}_k'' + 2\frac{z'}{z}\mathcal{R}_k' + c_s^2 k^2 \mathcal{R}_k = 0, \quad (4.7)$$

where now

$$\frac{z'}{z} = aH(1 + \epsilon - \delta - s), \quad (4.8)$$

with the prime corresponding to derivatives along conformal time τ . The slow-roll parameters are defined as

$$\epsilon = -\frac{\dot{H}}{H^2}, \quad \delta = -\frac{\ddot{H}}{2H\dot{H}}, \quad s = \frac{\dot{c}_s}{Hc_s}. \quad (4.9)$$

At this point, we can generalise the arguments we introduced in Section 2, where we have seen that the spectrum of curvature fluctuations can be enhanced at small scales

²⁰The implications of a smaller than unity speed of sound for the cosmological observables (n_s, r, α_s) in a model independent large- N approach was studied in [86], while frameworks to study large deviations from a slow-roll regime in similar contexts were developed in [87–89].

by violating the slow-roll conditions and changing the sign in the quantity z'/z (see the discussion around eq. (2.8)). In the case of non-canonical kinetic terms, we have one additional quantity to use – the parameter s which can turn large – and hence novel possibilities for producing PBHs. A full analysis of the phenomenological consequences of models based on this approach goes outside the scope of this paper: we limit ourselves to illustrating the effect of a varying speed of sound in a representative example.

4.2 Enhancement of curvature fluctuations in DBI inflation

The most famous example of inflation with non-standard kinetic terms motivated by string theory is Dirac-Born-Infeld (DBI) inflation [26, 27]. In this scenario, a probe D3-brane moves in the warped throat of a flux compactification in type IIB string theory. The dynamics is described by the DBI and Wess-Zumino actions, which give rise to:

$$P(X, \phi) = \frac{1}{h(\phi)}(1 - \gamma^{-1}) - V(\phi), \quad (4.10)$$

where $h(\phi)$ is the warp factor, which depends only on ϕ , and γ is defined as

$$\gamma^{-2} = 1 + 2Xh(\phi). \quad (4.11)$$

In this set-up, the speed of sound $c_s^2 = \gamma^{-2}$. Using (4.5), we find that the energy density is given by:

$$\rho = \frac{1}{h(\phi)}(\gamma - 1) + V(\phi). \quad (4.12)$$

We now consider what realisations of DBI setups can exhibit a transiently large slow-roll parameter s , which as we have observed can change the sign of the quantity z'/z (4.8) in the eq (4.7) governing the curvature perturbation, driving a growth in the latter. A large value for s can be induced by systems where the warp factor experienced by the moving D-brane has features [28, 29]. In particular, given that $c_s = 1/\gamma = \sqrt{1 - h(\phi)\dot{\phi}^2}$, a large $s = \dot{c}_s/(c_s H)$ could be achieved if $h(\phi)$ has a sharp decline. Such a feature in the warp factor could arise, for instance, if the D-brane that drives inflation travels down a double warped throat, sourced by two separated stacks of D-branes/localised fluxes [31, 32]. Another possibility is that during the DBI-brane's journey through the warped throat, some D-branes or flux at the bottom of the throat annihilate with some \bar{D} -branes, either perturbatively via D-brane- \bar{D} -brane annihilation, or non-perturbatively via the KPВ instability [33], thus reducing the strength of the warp factor.

We model these features by adding a step into an adS warp factor (though it would be important to understand more accurately how to realistically describe transitions in the warped geometry):

$$h(\phi) = \frac{a\lambda}{(\phi/\phi_0 + 1/2)^4} - \frac{b\lambda}{(\phi/\phi_0 + 1/2)^4} \left(1 - \frac{1}{1 + e^{-c(\phi/\phi_0 - d)}} \right). \quad (4.13)$$

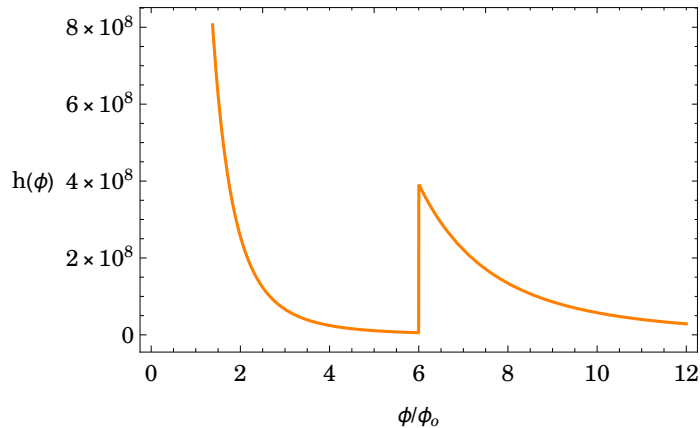


Figure 12. Warp factor $h(\phi)$ (4.13) as a function of ϕ/ϕ_0 for the following parameter choices $\lambda = 10^{10}$, $a = 70$, $b = 69$, $c = 2000$, $d = 6$.

This can be seen as a finite tip version of an adS warp factor with a step feature. The parameters a, b, c, d, λ , and ϕ_0 are constants expressed in appropriate units. We plot this warp factor in Figure 12. For simplicity, we will further assume a quadratic scalar potential:

$$V(\phi) = \frac{1}{2}m^2\phi^2. \quad (4.14)$$

As the D3-brane moves down the throat, it encounters a step downwards in the warp factor. This step produces a sharp increase in the speed of sound, c_s , and thus a large, positive value for s . So long as ϵ, δ remain smaller than s , there will be a region where $z'/z < 0$. This gives rise to a large driving term in the equation governing the curvature perturbation (4.7), and an expected growth in the superhorizon curvature perturbation. Indeed the parameters in our model can easily be chosen to produce a transiently large and negative value for z'/z , and we give an illustrative example in Figures 13-14.

Note that this proposal is distinct from the one we made in Section 3, in particular here there is no phase of ultra slow-roll, rather ϵ increases through the feature. Also, compared to the models presented in Section 3, $\delta < 0$ and therefore z'/z becomes negative due solely to the large positive value of s . Moreover z'/z is negative for a much briefer time (in e-folds), but it can also be much more negative; thus here we have a much stronger driving force for a much briefer period of time. Given the technical challenges in performing a complete numerical analysis for the cosmological perturbations in the present model with non-canonical kinetic terms including a sharp feature, we postpone this for future work. However, the heuristic arguments presented here and in Sections 2 and 3.5 suggest that an amplification of power in superhorizon modes can be achieved, and that this could provide a novel mechanism to produce interesting populations of PBHs.

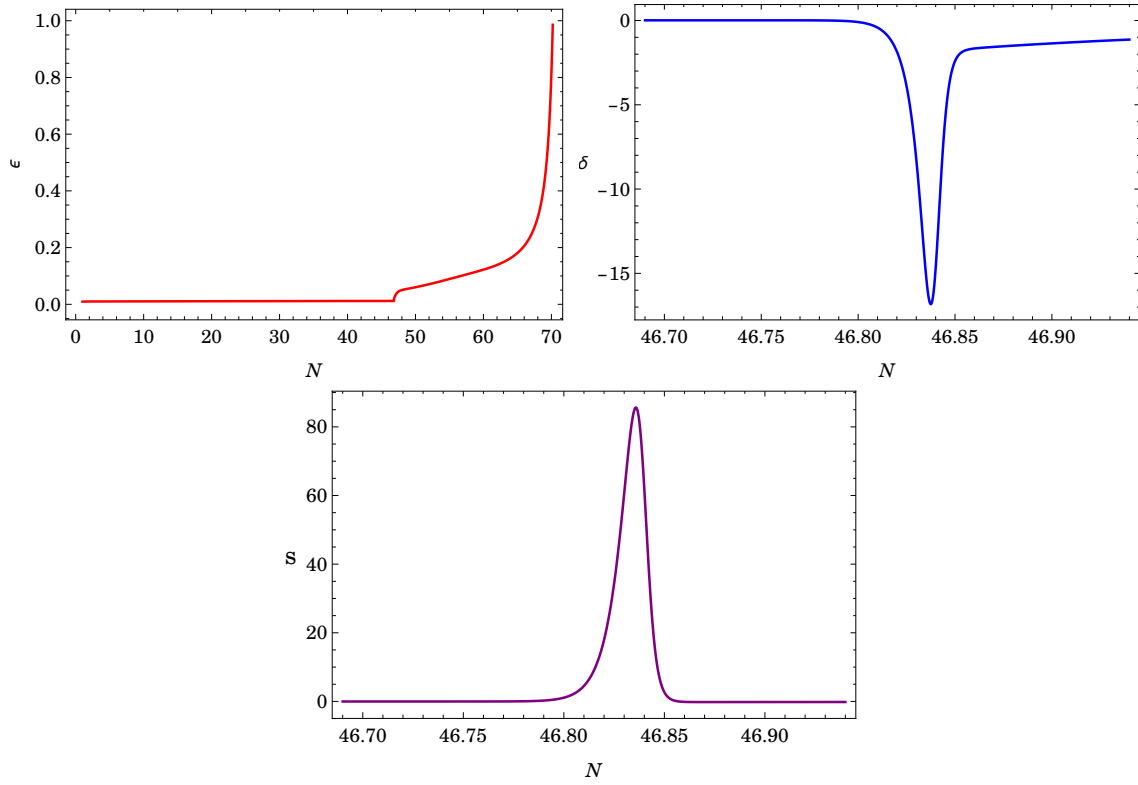


Figure 13. Slow-roll parameters ϵ, δ and s as a function e-folds N during DBI inflation for $\lambda = 10^{10}$, $a = 70$, $b = 69$, $c = 2000$, $d = 6$.

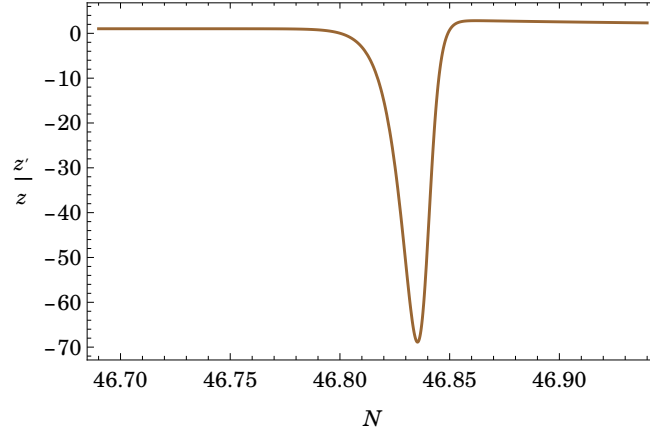


Figure 14. The behavior of z'/z in units of the comoving horizon size $(aH)^{-1}$ around the step like feature in the warp factor. The parameter choices are the same as in Figure 13.

5 Conclusions

In this paper, we present two well-motivated string theory scenarios which could give rise to a significant production of primordial black holes. If observed, these primordial black holes would not only provide an explanation for the nature of some or all of the Dark Matter that dominates cosmic structures, but also provide another window into the early Universe, looking onto a period of the inflationary epoch unseen by the CMB. Our interest in the current work has been in the production of PBHs around the mass scale $10^{17} - 10^{18}$ g ($10^{-16} - 10^{-15} M_\odot$), which can contribute a significant fraction of Dark Matter whilst evading current observational bounds. For such a PBH population, the amplitude of primordial density perturbations at the scales of interest ($k \sim 10^{13} \text{ Mpc}^{-1}$) should be around $A_s \sim 10^{-2}$, whilst the CMB observations set the amplitude at 10^{-9} for scales around $k_* \sim 0.05 \text{ Mpc}^{-1}$. Therefore, PBH Dark Matter requires that the inflationary potential has some distinct behaviour between CMB and PBH scales, which ultimately should be explained within the underlying fundamental theory.

A simple mechanism to enhance the amplitude of curvature perturbations during inflation within field theory models was identified by Leach et al [13, 14]. The idea is that perturbations on super-horizon scales can undergo a large amplification when the slow-roll approximation does not apply. Indeed, the equation governing the Fourier modes of the curvature perturbation takes the form of a damped harmonic oscillator:

$$\mathcal{R}_k'' + 2\frac{z'}{z}\mathcal{R}_k' + k^2\mathcal{R}_k = 0, \quad (5.1)$$

where $z \equiv a\dot{\phi}/H$. When the slow-roll approximation is a good one, around horizon crossing the dynamics are dominated by the friction term:

$$\frac{z'}{z} = aH(1 + \epsilon - \delta) \quad (5.2)$$

and the solution is well-approximated by \mathcal{R}_k constant, the growing adiabatic mode. But if the slow-roll approximation temporarily breaks down – in particular if $\delta > 1 + \epsilon$ – then the friction term can momentarily change to a driving term, leading to an amplification of the modes that have recently left the horizon. This may occur, for instance, when the potential has a region that is too steep to sustain slow-roll inflation and/or transitions to a region so flat that it supports an ultra slow-roll inflation. We consider ways within string theory to realise this idea and produce in particular sufficient amplification at the right scales to produce PBH Dark Matter.

Our first example is given by string axion inflation, including significant but subleading non-perturbative corrections which add bumps to the leading monomial axion potential. In earlier work, we showed that such effects can put axion inflation back into the favour of CMB observations, and here we note that they can moreover lead to an enhancement

of power in the curvature perturbations at smaller scales. Indeed, after CMB scales, the inflaton continues to roll down its bumpy potential through cliffs and plateaus towards its global minimum. The sub-leading corrections can be such that successive plateaus are shallower and shallower until a local minimum, inflection point and maximum emerges. As the inflaton traverses the local minimum climbing up the hill and passing through the inflection point, it undergoes a large deceleration, such that the second slow-roll parameter breaks the slow-roll condition, $\delta < 1$. Subsequently, the system enters a phase of “ultra slow-roll” inflation, with first slow-roll parameter dramatically suppressed $\epsilon \sim e^{-(2\delta)N}$ while $\delta \gtrsim 3$. It is also possible that the cliff preceding the local minimum is so steep that it can lead to a temporary interruption of inflation, where ϵ surpasses unity on the cliff before the rapid deceleration due to the inflection point.

We perform a numerical analysis of the linearized cosmological perturbations in our string-motivated model, using the MultiModeCode, and find the expected amplification of the curvature perturbation, in concordance with the heuristic arguments from [13, 14]. This result for the primordial power spectrum can then be used to estimate the present day PBH abundance. The fairly sharp peak in the curvature power spectrum leads to a fairly monochromatic PBH population. The five parameters in our model can be adjusted such that the CMB observables are within 2σ of the Planck data, and the mass and abundance of PBHs provide an order one fraction of the Dark Matter energy density. We also considered the implications of our scenario on the reheating epoch: for some – but not all – viable parameter choices an exotic post-inflationary equation of state is required. In addition to the population of light PBHs, potential signatures of such a scenario include a tensor-to-scalar ratio in the CMB of order $r \approx 10^{-3} - 10^{-2}$ and a large negative running of the spectral index.

The second way to amplify the super-horizon curvature perturbations that we present is found within the class of DBI inflation. Extending the Leach et al. argument to the case of DBI inflation, with a non-canonical kinetic term for the inflaton, reveals an additional contribution to the friction term in the mode equation:

$$\frac{z'}{z} = aH(1 + \epsilon - \delta - s) \quad \text{where} \quad s = \frac{\dot{c}_s}{Hc_s}. \quad (5.3)$$

The speed of sound in DBI inflation is determined by the warp factor, $c_s = 1/\gamma = \sqrt{1 - h(\phi)\dot{\phi}^2}$. Therefore, a steep downward step in the warp factor can lead to a large and positive \dot{c}_s , which transforms the friction term to a driving term and can thus potentially amplify the power in the super-horizon curvature mode. For example, this feature in the warp factor may occur due to geometrical effects such as a throat within a throat, sourced by two separated stacks of D-branes [31, 32]. Alternatively, a throat sourced by D-branes and/or fluxes would suffer an instability in the presence of \bar{D} -branes at its tip, due to perturbative brane-antibrane or non-perturbative flux-antibrane [33] annihilation. If the

system underwent this instability towards less warping at some time during the inflationary trajectory, this would have interesting consequences on the inflationary perturbations.

In the current paper, we model such phenomena by introducing a (smoothed) step-function into the warp factor. By solving numerically the background field equations through this feature, we show that indeed it can lead to a driving term in the mode equation and propose that this could lead to significant enhancement of amplitude in the curvature power spectrum at corresponding late small scales. Note that this would be distinct to previous scenarios in the literature, as there is no epoch of ultra-slow roll, rather ϵ increases through the feature. Due to the technical challenges in solving for the cosmological perturbations in this model with a non-canonical kinetic term with sharp feature, we postpone a detailed numerical analysis for future work. However, a rough quantitative analysis of the behaviour of the curvature perturbation modes through the feature as in [13, 14], supports the possibility that such a setup could provide a novel realisation of power enhancement in the primordial curvature perturbations and thus an interesting mechanism to produce PBHs.

Aside from a detailed numerical study of perturbations in our DBI model, there remain several interesting open questions. Our analysis on the dynamics in this work has been focused on the classical trajectory of the inflaton. However, in the region where inflaton experiences a strong deceleration, quantum fluctuations of the inflaton may dominate over extremely slow classical trajectory. In the slow-roll approximation, a recent analysis on this issue indeed show that quantum fluctuations can play a significant role in the estimates of PBH population [91]. Therefore, it would be interesting to study in some detail the role of these quantum fluctuations during the bumpy axion inflation we propose here, especially around the shallow minimum where slow-roll approximation breaks down. Another issue under current discussion is the impact of non-Gaussianities in the density perturbations on the PBH abundances.

Specific to our string-inspired models, it would be important to model more accurately the features in the warp factor that can arise in string compactifications. Although in principle the parameters $\{f, \Lambda_i, m\}$ of the axion model (3.2) (or $\{c, d\}$ in the DBI model (4.13)) could be tuned to adjust the position of the inflection point and produce a large population of PBH in the LIGO band ($M = 10 - 100M_\odot$), we could not find a viable parameter space that simultaneously produces a large peak in the scalar power spectrum and agrees with the CMB observations. It could be interesting to pursue this possibility by focusing on other axionic potentials that might arise in string theory constructions which we will leave for future work. Moreover, an intriguing possibility is that multiple features in the potential or speed of sound might allow for multiple monochromatic populations of PBHs, thus helping to evade current observational bounds and provide sufficient abundances to explain all of Dark Matter. Another interesting prospect is the possibility of an observable stochastic gravitational wave (GW) background associated with the scales related to the PBH formation, *e.g.* sourced at second order by the large scalar perturbations (see also

[92–96] for GW’s sourced by amplified vector fields) which seed the PBHs [97, 98].

To summarise, we have shown that string inflationary models are rich enough to match CMB observations and produce PBH populations with masses $\sim 10^{-16} - 10^{-15} M_{\odot}$ sufficient to explain Dark Matter. Bounds on PBHs are consistently improving. If such PBHs are observed in the future – and note there are no known astrophysical mechanisms to produce black holes in this mass range – they could not only explain the nature of Dark Matter but give invaluable information into the inflationary epoch. Together with observables such as the tensor-to-scalar ratio, the running of the spectral indices and non-Gaussianities in the CMB, it could be possible to further narrow down the stringy mechanisms at play during the inflationary epoch.

Acknowledgments

OÖ, GT and IZ are partially supported by the STFC grant ST/P00055X/1. SP thanks to the Swansea University Physics Department for its hospitality during the initial stages of this project.

References

- [1] S. Hawking, “Gravitationally collapsed objects of very low mass,” *Mon. Not. Roy. Astron. Soc.* **152** (1971) 75.
- [2] B. J. Carr and S. W. Hawking, “Black holes in the early Universe,” *Mon. Not. Roy. Astron. Soc.* **168** (1974) 399–415.
- [3] B. Carr, F. Kuhnel, and M. Sandstad, “Primordial Black Holes as Dark Matter,” *Phys. Rev.* **D94** no. 8, (2016) 083504, [arXiv:1607.06077 \[astro-ph.CO\]](#).
- [4] M. Sasaki, T. Suyama, T. Tanaka, and S. Yokoyama, “Primordial black holes—perspectives in gravitational wave astronomy,” *Class. Quant. Grav.* **35** no. 6, (2018) 063001, [arXiv:1801.05235 \[astro-ph.CO\]](#).
- [5] J. Garcia-Bellido, A. D. Linde, and D. Wands, “Density perturbations and black hole formation in hybrid inflation,” *Phys. Rev.* **D54** (1996) 6040–6058, [arXiv:astro-ph/9605094 \[astro-ph\]](#).
- [6] F. Capela, M. Pshirkov, and P. Tinyakov, “Adiabatic contraction revisited: implications for primordial black holes,” *Phys. Rev.* **D90** no. 8, (2014) 083507, [arXiv:1403.7098 \[astro-ph.CO\]](#).
- [7] J. Garcia-Bellido and E. Ruiz Morales, “Primordial black holes from single field models of inflation,” *Phys. Dark Univ.* **18** (2017) 47–54, [arXiv:1702.03901 \[astro-ph.CO\]](#).
- [8] J. M. Ezquiaga, J. Garcia-Bellido, and E. Ruiz Morales, “Primordial Black Hole production in Critical Higgs Inflation,” *Phys. Lett.* **B776** (2018) 345–349, [arXiv:1705.04861 \[astro-ph.CO\]](#).

- [9] G. Ballesteros and M. Taoso, “Primordial black hole dark matter from single field inflation,” *Phys. Rev.* **D97** no. 2, (2018) 023501, [arXiv:1709.05565 \[hep-ph\]](#).
- [10] M. P. Hertzberg and M. Yamada, “Primordial Black Holes from Polynomial Potentials in Single Field Inflation,” [arXiv:1712.09750 \[astro-ph.CO\]](#).
- [11] K. Kannike, L. Marzola, M. Raidal, and H. Veermäe, “Single Field Double Inflation and Primordial Black Holes,” *JCAP* **1709** no. 09, (2017) 020, [arXiv:1705.06225 \[astro-ph.CO\]](#).
- [12] M. Cicoli, V. A. Diaz, and F. G. Pedro, “Primordial Black Holes from String Inflation,” [arXiv:1803.02837 \[hep-th\]](#).
- [13] S. M. Leach and A. R. Liddle, “Inflationary perturbations near horizon crossing,” *Phys. Rev.* **D63** (2001) 043508, [arXiv:astro-ph/0010082 \[astro-ph\]](#).
- [14] S. M. Leach, M. Sasaki, D. Wands, and A. R. Liddle, “Enhancement of superhorizon scale inflationary curvature perturbations,” *Phys. Rev.* **D64** (2001) 023512, [arXiv:astro-ph/0101406 \[astro-ph\]](#).
- [15] A. A. Starobinsky, “Spectrum of adiabatic perturbations in the universe when there are singularities in the inflation potential,” *JETP Lett.* **55** (1992) 489–494. [Pisma Zh. Eksp. Teor. Fiz.55,477(1992)].
- [16] X. Chen, H. Firouzjahi, M. H. Namjoo, and M. Sasaki, “A Single Field Inflation Model with Large Local Non-Gaussianity,” *EPL* **102** no. 5, (2013) 59001, [arXiv:1301.5699 \[hep-th\]](#).
- [17] S. Parameswaran, G. Tasinato, and I. Zavala, “Subleading Effects and the Field Range in Axion Inflation,” *JCAP* **1604** no. 04, (2016) 008, [arXiv:1602.02812 \[astro-ph.CO\]](#).
- [18] A. Linde, S. Mooij, and E. Pajer, “Gauge field production in supergravity inflation: Local non-Gaussianity and primordial black holes,” *Phys. Rev.* **D87** no. 10, (2013) 103506, [arXiv:1212.1693 \[hep-th\]](#).
- [19] E. Bugaev and P. Klimai, “Axion inflation with gauge field production and primordial black holes,” *Phys. Rev.* **D90** no. 10, (2014) 103501, [arXiv:1312.7435 \[astro-ph.CO\]](#).
- [20] J. Garcia-Bellido, M. Peloso, and C. Unal, “Gravitational waves at interferometer scales and primordial black holes in axion inflation,” *JCAP* **1612** no. 12, (2016) 031, [arXiv:1610.03763 \[astro-ph.CO\]](#).
- [21] V. Domcke, M. Pieroni, and P. Binétruy, “Primordial gravitational waves for universality classes of pseudoscalar inflation,” *JCAP* **1606** (2016) 031, [arXiv:1603.01287 \[astro-ph.CO\]](#).
- [22] S.-L. Cheng, W. Lee, and K.-W. Ng, “Primordial black holes and associated gravitational waves in axion monodromy inflation,” [arXiv:1801.09050 \[astro-ph.CO\]](#).
- [23] E. Silverstein and A. Westphal, “Monodromy in the CMB: Gravity Waves and String Inflation,” *Phys. Rev.* **D78** (2008) 106003, [arXiv:0803.3085 \[hep-th\]](#).

- [24] L. McAllister, E. Silverstein, and A. Westphal, “Gravity Waves and Linear Inflation from Axion Monodromy,” *Phys.Rev.* **D82** (2010) 046003, [arXiv:0808.0706 \[hep-th\]](#).
- [25] K. Freese, J. A. Frieman, and A. V. Olinto, “Natural inflation with pseudo - Nambu-Goldstone bosons,” *Phys.Rev.Lett.* **65** (1990) 3233–3236.
- [26] E. Silverstein and D. Tong, “Scalar speed limits and cosmology: Acceleration from D-cceleration,” *Phys. Rev.* **D70** (2004) 103505, [arXiv:hep-th/0310221 \[hep-th\]](#).
- [27] M. Alishahiha, E. Silverstein, and D. Tong, “DBI in the sky,” *Phys. Rev.* **D70** (2004) 123505, [arXiv:hep-th/0404084 \[hep-th\]](#).
- [28] R. Bean, X. Chen, G. Hailu, S. H. H. Tye, and J. Xu, “Duality Cascade in Brane Inflation,” *JCAP* **0803** (2008) 026, [arXiv:0802.0491 \[hep-th\]](#).
- [29] V. Miranda, W. Hu, and P. Adshead, “Warp Features in DBI Inflation,” *Phys. Rev.* **D86** (2012) 063529, [arXiv:1207.2186 \[astro-ph.CO\]](#).
- [30] G. Hailu and S. H. H. Tye, “Structures in the Gauge/Gravity Duality Cascade,” *JHEP* **08** (2007) 009, [arXiv:hep-th/0611353 \[hep-th\]](#).
- [31] S. Franco, A. Hanany, and A. M. Uranga, “Multi-flux warped throats and cascading gauge theories,” *JHEP* **09** (2005) 028, [arXiv:hep-th/0502113 \[hep-th\]](#).
- [32] J. F. G. Cascales, F. Saad, and A. M. Uranga, “Holographic dual of the standard model on the throat,” *JHEP* **11** (2005) 047, [arXiv:hep-th/0503079 \[hep-th\]](#).
- [33] S. Kachru, J. Pearson, and H. L. Verlinde, “Brane / flux annihilation and the string dual of a nonsupersymmetric field theory,” *JHEP* **06** (2002) 021, [arXiv:hep-th/0112197 \[hep-th\]](#).
- [34] T. Kobayashi, A. Oikawa, and H. Otsuka, “New potentials for string axion inflation,” *Phys. Rev.* **D93** no. 8, (2016) 083508, [arXiv:1510.08768 \[hep-ph\]](#).
- [35] N. Cabo Bizet, O. Loaiza-Brito, and I. Zavala, “Mirror quintic vacua: hierarchies and inflation,” *JHEP* **10** (2016) 082, [arXiv:1605.03974 \[hep-th\]](#).
- [36] R. Kallosh, A. Linde, and B. Vercnocke, “Natural Inflation in Supergravity and Beyond,” *Phys. Rev.* **D90** no. 4, (2014) 041303, [arXiv:1404.6244 \[hep-th\]](#).
- [37] R. Flauger, L. McAllister, E. Silverstein, and A. Westphal, “Drifting Oscillations in Axion Monodromy,” *JCAP* **1710** no. 10, (2017) 055, [arXiv:1412.1814 \[hep-th\]](#).
- [38] T. Banks, M. Dine, P. J. Fox, and E. Gorbatov, “On the possibility of large axion decay constants,” *JCAP* **0306** (2003) 001, [arXiv:hep-th/0303252 \[hep-th\]](#).
- [39] W. H. Kinney, “Horizon crossing and inflation with large eta,” *Phys. Rev.* **D72** (2005) 023515, [arXiv:gr-qc/0503017 \[gr-qc\]](#).
- [40] J. Martin, H. Motohashi, and T. Suyama, “Ultra Slow-Roll Inflation and the non-Gaussianity Consistency Relation,” *Phys. Rev.* **D87** no. 2, (2013) 023514, [arXiv:1211.0083 \[astro-ph.CO\]](#).
- [41] C. Germani and T. Prokopec, “On primordial black holes from an inflection point,” *Phys.*

- Dark Univ.* **18** (2017) 6–10, [arXiv:1706.04226](#) [[astro-ph.CO](#)].
- [42] K. Dimopoulos, “Ultra slow-roll inflation demystified,” *Phys. Lett.* **B775** (2017) 262–265, [arXiv:1707.05644](#) [[hep-ph](#)].
- [43] H. Motohashi and W. Hu, “Primordial Black Holes and Slow-Roll Violation,” *Phys. Rev.* **D96** no. 6, (2017) 063503, [arXiv:1706.06784](#) [[astro-ph.CO](#)].
- [44] E. D. Stewart and D. H. Lyth, “A More accurate analytic calculation of the spectrum of cosmological perturbations produced during inflation,” *Phys. Lett.* **B302** (1993) 171–175, [arXiv:gr-qc/9302019](#) [[gr-qc](#)].
- [45] R. Easther and H. Peiris, “Implications of a Running Spectral Index for Slow Roll Inflation,” *JCAP* **0609** (2006) 010, [arXiv:astro-ph/0604214](#) [[astro-ph](#)].
- [46] D. H. Lyth and A. R. Liddle, *The primordial density perturbation: Cosmology, inflation and the origin of structure*. 2009. <http://www.cambridge.org/uk/catalogue/catalogue.asp?isbn=9780521828499>.
- [47] **Planck** Collaboration, P. Ade *et al.*, “Planck 2015 results. XX. Constraints on inflation,” [arXiv:1502.02114](#) [[astro-ph.CO](#)].
- [48] M. J. Mortonson, H. V. Peiris, and R. Easther, “Bayesian Analysis of Inflation: Parameter Estimation for Single Field Models,” *Phys. Rev.* **D83** (2011) 043505, [arXiv:1007.4205](#) [[astro-ph.CO](#)].
- [49] R. Easther and H. V. Peiris, “Bayesian Analysis of Inflation II: Model Selection and Constraints on Reheating,” *Phys. Rev.* **D85** (2012) 103533, [arXiv:1112.0326](#) [[astro-ph.CO](#)].
- [50] J. Norena, C. Wagner, L. Verde, H. V. Peiris, and R. Easther, “Bayesian Analysis of Inflation III: Slow Roll Reconstruction Using Model Selection,” *Phys. Rev.* **D86** (2012) 023505, [arXiv:1202.0304](#) [[astro-ph.CO](#)].
- [51] R. Easther, J. Frazer, H. V. Peiris, and L. C. Price, “Simple predictions from multifield inflationary models,” *Phys. Rev. Lett.* **112** (2014) 161302, [arXiv:1312.4035](#) [[astro-ph.CO](#)].
- [52] L. C. Price, H. V. Peiris, J. Frazer, and R. Easther, “Gravitational wave consistency relations for multifield inflation,” *Phys. Rev. Lett.* **114** no. 3, (2015) 031301, [arXiv:1409.2498](#) [[astro-ph.CO](#)].
- [53] L. C. Price, J. Frazer, J. Xu, H. V. Peiris, and R. Easther, “MultiModeCode: An efficient numerical solver for multifield inflation,” *JCAP* **1503** no. 03, (2015) 005, [arXiv:1410.0685](#) [[astro-ph.CO](#)].
- [54] T. Kobayashi and F. Takahashi, “Running Spectral Index from Inflation with Modulations,” *JCAP* **1101** (2011) 026, [arXiv:1011.3988](#) [[astro-ph.CO](#)].
- [55] **CMB-S4** Collaboration, K. N. Abazajian *et al.*, “CMB-S4 Science Book, First Edition,” [arXiv:1610.02743](#) [[astro-ph.CO](#)].

- [56] B. J. Carr, “The Primordial black hole mass spectrum,” *Astrophys. J.* **201** (1975) 1–19.
- [57] P. Ivanov, P. Naselsky, and I. Novikov, “Inflation and primordial black holes as dark matter,” *Phys. Rev.* **D50** (1994) 7173–7178.
- [58] T. Nakama, J. Silk, and M. Kamionkowski, “Stochastic gravitational waves associated with the formation of primordial black holes,” *Phys. Rev.* **D95** no. 4, (2017) 043511, [arXiv:1612.06264 \[astro-ph.CO\]](#).
- [59] W. H. Press and P. Schechter, “Formation of galaxies and clusters of galaxies by selfsimilar gravitational condensation,” *Astrophys. J.* **187** (1974) 425–438.
- [60] P. Pina Avelino, “Primordial black hole constraints on non-gaussian inflation models,” *Phys. Rev.* **D72** (2005) 124004, [arXiv:astro-ph/0510052 \[astro-ph\]](#).
- [61] S. Young and C. T. Byrnes, “Primordial black holes in non-Gaussian regimes,” *JCAP* **1308** (2013) 052, [arXiv:1307.4995 \[astro-ph.CO\]](#).
- [62] Y. Tada and S. Yokoyama, “Primordial black holes as biased tracers,” *Phys. Rev.* **D91** no. 12, (2015) 123534, [arXiv:1502.01124 \[astro-ph.CO\]](#).
- [63] S. Young and C. T. Byrnes, “Signatures of non-gaussianity in the isocurvature modes of primordial black hole dark matter,” *JCAP* **1504** no. 04, (2015) 034, [arXiv:1503.01505 \[astro-ph.CO\]](#).
- [64] S. Young, D. Regan, and C. T. Byrnes, “Influence of large local and non-local bispectra on primordial black hole abundance,” *JCAP* **1602** no. 02, (2016) 029, [arXiv:1512.07224 \[astro-ph.CO\]](#).
- [65] G. Franciolini, A. Kehagias, S. Matarrese, and A. Riotto, “Primordial Black Holes from Inflation and non-Gaussianity,” [arXiv:1801.09415 \[astro-ph.CO\]](#).
- [66] J. M. Maldacena, “Non-Gaussian features of primordial fluctuations in single field inflationary models,” *JHEP* **05** (2003) 013, [arXiv:astro-ph/0210603](#).
- [67] M. H. Namjoo, H. Firouzjahi, and M. Sasaki, “Violation of non-Gaussianity consistency relation in a single field inflationary model,” *EPL* **101** no. 3, (2013) 39001, [arXiv:1210.3692 \[astro-ph.CO\]](#).
- [68] Y.-F. Cai, X. Chen, M. H. Namjoo, M. Sasaki, D.-G. Wang, and Z. Wang, “Revisiting non-Gaussianity from non-attractor inflation models,” [arXiv:1712.09998 \[astro-ph.CO\]](#).
- [69] R. Bravo, S. Mooij, G. A. Palma, and B. Pradenas, “Vanishing of local non-Gaussianity in canonical single field inflation,” [arXiv:1711.05290 \[astro-ph.CO\]](#).
- [70] S. Young, C. T. Byrnes, and M. Sasaki, “Calculating the mass fraction of primordial black holes,” *JCAP* **1407** (2014) 045, [arXiv:1405.7023 \[gr-qc\]](#).
- [71] K. Inomata, M. Kawasaki, K. Mukaida, Y. Tada, and T. T. Yanagida, “Inflationary Primordial Black Holes as All Dark Matter,” *Phys. Rev.* **D96** no. 4, (2017) 043504, [arXiv:1701.02544 \[astro-ph.CO\]](#).

- [72] T. Harada, C.-M. Yoo, and K. Kohri, “Threshold of primordial black hole formation,” *Phys. Rev.* **D88** no. 8, (2013) 084051, [arXiv:1309.4201 \[astro-ph.CO\]](#). [Erratum: *Phys. Rev.* **D89**,no.2,029903(2014)].
- [73] I. Musco and J. C. Miller, “Primordial black hole formation in the early universe: critical behaviour and self-similarity,” *Class. Quant. Grav.* **30** (2013) 145009, [arXiv:1201.2379 \[gr-qc\]](#).
- [74] A. Gould, “Femtolensing of gamma-ray bursters,” *The Astrophysical Journal* **386** (1992) L5–L7.
- [75] A. Barnacka, J. F. Glicenstein, and R. Moderski, “New constraints on primordial black holes abundance from femtolensing of gamma-ray bursts,” *Phys. Rev.* **D86** (2012) 043001, [arXiv:1204.2056 \[astro-ph.CO\]](#).
- [76] B. Carr, M. Raidal, T. Tenkanen, V. Vaskonen, and H. Veermäe, “Primordial black hole constraints for extended mass functions,” *Phys. Rev.* **D96** no. 2, (2017) 023514, [arXiv:1705.05567 \[astro-ph.CO\]](#).
- [77] A. R. Liddle and S. M. Leach, “How long before the end of inflation were observable perturbations produced?,” *Phys.Rev.* **D68** (2003) 103503, [arXiv:astro-ph/0305263 \[astro-ph\]](#).
- [78] P. Adshead, R. Easther, J. Pritchard, and A. Loeb, “Inflation and the Scale Dependent Spectral Index: Prospects and Strategies,” *JCAP* **1102** (2011) 021, [arXiv:1007.3748 \[astro-ph.CO\]](#).
- [79] A. Maharana and I. Zavala, “Post-inflationary Scalar Tensor Cosmology and Inflationary Parameters,” [arXiv:1712.07071 \[hep-ph\]](#).
- [80] M. Joyce, “Electroweak Baryogenesis and the Expansion Rate of the Universe,” *Phys. Rev.* **D55** (1997) 1875–1878, [arXiv:hep-ph/9606223 \[hep-ph\]](#).
- [81] P. G. Ferreira and M. Joyce, “Cosmology with a primordial scaling field,” *Phys. Rev.* **D58** (1998) 023503, [arXiv:astro-ph/9711102 \[astro-ph\]](#).
- [82] R. Easther, R. Galvez, O. Özsoy, and S. Watson, “Supersymmetry, Nonthermal Dark Matter and Precision Cosmology,” *Phys. Rev.* **D89** no. 2, (2014) 023522, [arXiv:1307.2453 \[hep-ph\]](#).
- [83] A. L. Erickcek and K. Sigurdson, “Reheating Effects in the Matter Power Spectrum and Implications for Substructure,” *Phys.Rev.* **D84** (2011) 083503, [arXiv:1106.0536 \[astro-ph.CO\]](#).
- [84] J. Fan, O. Özsoy, and S. Watson, “Nonthermal histories and implications for structure formation,” *Phys. Rev.* **D90** no. 4, (2014) 043536, [arXiv:1405.7373 \[hep-ph\]](#).
- [85] A. L. Erickcek, “The Dark Matter Annihilation Boost from Low-Temperature Reheating,” *Phys. Rev.* **D92** no. 10, (2015) 103505, [arXiv:1504.03335 \[astro-ph.CO\]](#).
- [86] I. Zavala, “Effects of the speed of sound at large-N,” *Phys. Rev.* **D91** no. 6, (2015) 063005, [arXiv:1412.3732 \[astro-ph.CO\]](#).

- [87] S. Renaux-Petel and G. Tasinato, “Nonlinear perturbations of cosmological scalar fields with non-standard kinetic terms,” *JCAP* **0901** (2009) 012, [arXiv:0810.2405 \[hep-th\]](#).
- [88] J. Emery, G. Tasinato, and D. Wands, “Local non-Gaussianity from rapidly varying sound speeds,” *JCAP* **1208** (2012) 005, [arXiv:1203.6625 \[hep-th\]](#).
- [89] J. Emery, G. Tasinato, and D. Wands, “Mixed non-Gaussianity in multiple-DBI inflation,” *JCAP* **1305** (2013) 021, [arXiv:1303.3975 \[astro-ph.CO\]](#).
- [90] J. Garriga and V. F. Mukhanov, “Perturbations in k-inflation,” *Phys. Lett.* **B458** (1999) 219–225, [arXiv:hep-th/9904176 \[hep-th\]](#).
- [91] C. Pattison, V. Vennin, H. Assadullahi, and D. Wands, “Quantum diffusion during inflation and primordial black holes,” *JCAP* **1710** no. 10, (2017) 046, [arXiv:1707.00537 \[hep-th\]](#).
- [92] J. L. Cook and L. Sorbo, “Particle production during inflation and gravitational waves detectable by ground-based interferometers,” [arXiv:1109.0022 \[astro-ph.CO\]](#).
- [93] N. Barnaby, J. Moxon, R. Namba, M. Peloso, G. Shiu, *et al.*, “Gravity waves and non-Gaussian features from particle production in a sector gravitationally coupled to the inflaton,” *Phys.Rev.* **D86** (2012) 103508, [arXiv:1206.6117 \[astro-ph.CO\]](#).
- [94] O. Özsoy, K. Sinha, and S. Watson, “How Well Can We Really Determine the Scale of Inflation?,” *Phys. Rev.* **D91** no. 10, (2015) 103509, [arXiv:1410.0016 \[hep-th\]](#).
- [95] R. Namba, M. Peloso, M. Shiraishi, L. Sorbo, and C. Unal, “Scale-dependent gravitational waves from a rolling axion,” *JCAP* **1601** no. 01, (2016) 041, [arXiv:1509.07521 \[astro-ph.CO\]](#).
- [96] O. Özsoy, “On Synthetic Gravitational Waves from Multi-field Inflation,” *JCAP* **1804** no. 04, (2018) 062, [arXiv:1712.01991 \[astro-ph.CO\]](#).
- [97] L. Alabidi, K. Kohri, M. Sasaki, and Y. Sendouda, “Observable induced gravitational waves from an early matter phase,” *JCAP* **1305** (2013) 033, [arXiv:1303.4519 \[astro-ph.CO\]](#).
- [98] J. Garcia-Bellido, M. Peloso, and C. Unal, “Gravitational Wave signatures of inflationary models from Primordial Black Hole Dark Matter,” *JCAP* **1709** no. 09, (2017) 013, [arXiv:1707.02441 \[astro-ph.CO\]](#).